

1 **Measurement report: Ambient volatile organic compounds (VOCs) pollution at urban**
2 **Beijing: characteristics, sources, and implications for pollution control**

3 Lulu Cui¹, Di Wu¹, Shuxiao Wang^{1,2*}, Qingcheng Xu¹, Ruolan Hu¹, Jiming Hao^{1,2}

4 ¹ *State Key Joint Laboratory of Environment Simulation and Pollution Control, School of Environment,*
5 *Tsinghua University, Beijing 100084, China*

6 ² *State Environmental Protection Key Laboratory of Sources and Control of Air Pollution Complex, Beijing*
7 *100084, China*

8 * Corresponding author. E-mail address: shxwang@tsinghua.edu.cn

9 **Abstract**

10 The increasing ozone (O₃) pollution and high fraction of secondary organic aerosols (SOA) in fine particle mass
11 highlighted the importance of volatile organic compounds (VOCs) in air pollution control. In this work, a
12 campaign of comprehensive field observations was conducted at an urban site in Beijing, from December 2018
13 to November 2019, to ~~identify characterize VOCs the composition, sources and their contributions to air~~
14 ~~pollution and secondary transformation potential of VOCs.~~ The total mixing ratio of the 95 quantified VOCs
15 (TVOC) observed in this study ranged from 5.5–118.7 ppbv with the mean value of 34.9 ppbv, ~~and the~~
16 ~~contemporaneous mixing ratios of TVOC was significantly lower than those observed in 2014 and 2016,~~
17 ~~confirming the effectiveness of VOCs emission control measures in Beijing in recent years.~~ Alkanes, OVOCs
18 and halocarbons were the dominant chemical groups, accounting for 75–81% of the TVOCs across the sampling
19 months. ~~High and low O₃/PM_{2.5} months as well as several O₃/PM_{2.5} polluted days were identified during the~~
20 ~~sampling period.~~ The molar ratios of VOCs to NO_x indicated that O₃ formation was limited by VOCs during the
21 whole sampling period. Positive matrix factorization (PMF) analysis showed that diesel vehicle exhaust, gasoline
22 vehicle exhaust and industrial emissions were the main VOCs sources during both the O₃-polluted and PM_{2.5}-

23 ~~polluted months. Diesel exhaust and industrial emission were identified as the major VOCs sources on both O₃-~~
24 ~~polluted and PM_{2.5}-polluted days based on positive matrix factorization (PMF) analysis, accounting for 46% and~~
25 ~~53%, respectively. Moreover, higher proportion of oil/gas evaporation was observed on O₃-polluted days (18%)~~
26 ~~than that on O₃-clean days (13%), and higher proportion of coal/biomass combustion was observed on PM_{2.5}-~~
27 ~~polluted days (18%) than that on PM_{2.5}-clean days (13%).~~ On the base of O₃ formation impact, VOCs from fuel
28 evaporation and diesel exhaust particularly toluene, xylenes, trans-2-butene, acrolein, methyl methacrylate, vinyl
29 acetate, 1-butene and 1-hexene were the main contributors, illustrating the necessity of conducting emission
30 controls on these pollution sources and species for alleviating O₃ pollution. Instead, VOCs from diesel exhaust
31 and coal/biomass combustion were found to be the dominant contributors for secondary organic aerosol
32 formation potential (SOAFP), particularly the VOC species of toluene, 1-hexene, xylenes, ethylbenzene and
33 styrene, and top priority should be given to these for the alleviation of haze pollution. ~~The positive matrix~~
34 ~~factorization (PSCF) analysis showed that O₃ and PM_{2.5} pollution was mainly affected by local emissions.~~ This
35 study provides insights for government to formulate effective VOCs control measures for air pollution in Beijing.

36 **Key words:** VOCs, OFP, SOAFP, Source appointment

37 **1. Introduction**

38 The ozone (O₃) and fine particulate matter (PM_{2.5}) pollution has restricted improvements in air quality in China.
39 Observation data from the Chinese Ministry of Environment and Ecology (MEE) network has witnessed an upward
40 trend for O₃ across the country over the period 2013-2019 (Fu et al., 2019; Li et al., 2017; Li et al., 2020; Shen
41 et al., 2019; Fan et al., 2020). Besides, haze pollution occurred in urban sites in recent years were commonly
42 characterized by high-enhanced fractions formation of secondary organic aerosols (SOA) in fine particles, e.g.,
43 the fraction of SOA in organic aerosols reached 58% in Xi'an during winter 2018 and 53% in urban Beijing
44 during winter 2014 (Guo et al., 2014; Huang et al., 2014; Kuang et al., 2020; Li et al., 2017b; Sun et al., 2020; Xu
45 et al., 2019). Volatile organic compounds (VOCs) are key precursors for the formation of O₃ via multiphase-gas-
46 phase reactions (Odum et al., 1997; Atkinson, 2000; Sato et al., 2010; Huang et al., 2014). In highly polluted
47 urban regions, the O₃ formation was generally VOCs-limited, and it is suggested that VOCs emission control is
48 necessary for effective alleviation of photochemical smog (Liu et al., 2020a,b; Shao et al., 2009; Wang et al.,
49 2020; Xing et al., 2011). Besides, the VOCs compounds including aromatics and biogenic species have
50 significant impact on SOA formation which play an important role in haze formation (Hallquist et al., 2009;
51 Huang et al., 2014; Tong et al., 2021). VOCs emission abatement is therefore imperative for improving air
52 quality in China.

53 VOCs in ambient air can be emitted by a variety of sources including both anthropogenic and biogenic
54 sources. While biogenic emissions are more-significantly greater than ~~10-times that of~~ anthropogenic emissions
55 globally (Roger and Janet, 2003; Doumbia et al., 2021; Sindelarova et al., 2022), anthropogenic emissions play
56 the dominant role in urban and surrounding areas (Warneke et al., 2007; Ahmad et al., 2017; Wu and Xie, 2018).
57 The VOC observations in China showed distinct differences in anthropogenic sources among different regions.

58 For example, solvent use and vehicle exhaust are primary VOCs sources in urban Shanghai and urban Guangzhou,
59 while the primary sources of VOCs in Wuhan, Zhengzhou and Beijing cities are combustion and vehicle exhaust
60 (Han et al., 2020; Shen et al., 2020; Liu et al., 2020a; Li et al., 2019a). Apart from the diversity of emission
61 sources, different VOCs species exhibited different propensities to form O₃ and SOA. Observation-based studies
62 commonly applied the O₃ formation potential (OFP) and SOA formation potential (SOAFP) scales to quantify
63 the relative effects of specific VOCs and sources on O₃ and SOA formation and to aid in the development of
64 efficient control strategies (Carter and Atkinson, 1989; Chang and Rudy, 1990; Han et al., 2020; Zhang et al.,
65 2017^a). Although there have been many studies on ambient VOCs in various locations (e.g., urban, rural, and
66 industrial areas), most of these measurements were confined to short periods (a few days or a certain season),
67 and the understanding of temporal variations of concentrations, sources as well as the influence of photochemical
68 reactions of VOCs on annual scale was still limited. Besides, most of the available reports on VOCs analysis
69 based on online analytical techniques include mainly non-methane hydrocarbon compounds, and thus the
70 characteristics of VOCs as well as their relationships with PM_{2.5} and O₃ cannot be fully revealed since OVOC
71 also participate actively in chemical reactions related to secondary formation (Li et al., 2019a; Zhao et al., 2020;
72 Yang et al., 2018; Sinha and Sinha., 2019). Therefore, the long-term and comprehensive monitoring of VOCs are
73 desired.

74 As the capital and one of the largest megacities in China, Beijing has been suffering from severe O₃ pollution
75 due to rapid economic development and increases in precursor emissions (Wang et al., 2014^a; Wang et al., 2017;
76 Li et al., 2019d; Zhao et al., 2020). According to the Report on the State of the Ecology and Environment in
77 Beijing, the average 90th percentile O₃ daily maximum 8 h concentration in Beijing exceeded the national
78 standards, reaching 193, 192, and 191 µg/m³ in 2017, 2018, and 2019, respectively. In addition, the number of

79 motor vehicles in Beijing reached 6.365 million at the end of 2019 (<http://beijing.gov.cn>), making Beijing the
80 top city in China in terms of number of motor vehicles. The existing field measurements in Beijing were mostly
81 conducted before 2016, and the observation in most recent years is quite limited (Li et al., 2015; Li et al., 2019c;
82 Liu et al., 2020a; Yang et al., 2018). In this work, a campaign of comprehensive field observations was conducted
83 at an urban site in Beijing during December 2018 and November 2019 for the analysis of VOCs. Several O₃ and
84 PM_{2.5} pollution events were captured during the sampling period. The characteristics and the contribution of
85 specific species and sources of VOCs on O₃ and SOA formation, with a focus on photochemical and haze
86 pollution periods, were analyzed in detail. The results and implications from this study can provide useful guidance
87 for policymakers to alleviate ozone and haze pollution in Beijing.

88 **2. Methodology**

89 **2.1 Field measurement**

90 The sampling site is at the roof of a three-floor building on the campus of Tsinghua University (40.00°N,
91 116.33°E), northwest of Beijing urban area (Fig. S1). The altitude of the sampling site is 57 m. This sampling
92 site is surrounded by school and there are no large emission sources nearby, therefore it can represent the urban
93 air quality in Beijing. Details of the site description is found in Xu et al., (2019).

94 The air samples were collected using 6 L summa canisters (Entech, USA) with a stable rate of 4.26 ml/min.
95 The samples were pre-processed to remove N₂, O₂, CO₂, CO and H₂O in the samples and to further concentrate
96 the samples in volume by the cryogenic pre-concentrator (Model 7100, Entech Instruments Inc., USA). Pressure
97 gage was used to test if the canister has air leakage exist before sampling every time, and blanks were prepared
98 using cleaned canisters to fill with high purity nitrogen. The cryotrap of precooling system was baked before
99 analyses each day and between every samples. The VOCs in air samples were analyzed by a gas chromatography

100 system that was equipped with a mass spectrometric detector (GC-MS) (Agilent Tech., 7890/5975, USA). The
101 availability of this system for VOCs measurement are well verified and it has been used in field campaigns (Li
102 et al., 2014; Wu et al., 2016). The column temperature was controlled by an initial temperature of -40 °C. The
103 programmed temperature was used with helium as carrier gas, and the flow rate was set at 1.5 ml min⁻¹. The
104 initial temperature was set at 90 °C, and then switched to 220 °C. In this work, 95 target VOCs, including 25
105 alkanes, 8 alkenes, 16 aromatics, 34 halocarbons and 12 OVOC were quantified. It should be noted that VOCs
106 compounds (C2-C3) with low boiling point (i.e., ethane, ethene, acetylene, and propane) were not detected by
107 the GC-MS system. The standard substance (SPECTRA GASES Inc., USA) mentioned for Photochemical
108 Assessment Monitoring Stations (PAMS) and US EPA TO-15 standard was used to construct the calibration
109 curves for the 95 target VOCs, ~~including 25 alkanes, 8 alkenes, 16 aromatics, 34 halocarbons and 12 OVOC.~~
110 Quality assurance and quality control, including method detection limit (MDL) of each compound, laboratory
111 and field blanks, retention time, accuracy and duplicate measurements of samples were performed according to
112 USEPA Compendium Method TO-15 (USEPA 1999). The correlated coefficients of the calibration curves for all
113 the compounds ~~was~~ were > 0.95. The relative standard deviation (RSD) for all of compounds of triplicates were
114 0.5%-6.0%. Previous field measurements have reported that the precision of GC-MS system for hydrocarbons
115 and aldehydes was below 6% and 15%, respectively (Li et al., 2014; Wu et al., 2016). In this work, one kind of
116 aldehyde substance, i.e., ethylacrolein was detected, with R² and RSD of 0.99 and 4.5%, respectively.

117 During the sampling periods, the measurements of PM_{2.5}, gaseous pollutants (NO_x and O₃), and
118 meteorological variables (such as temperature, relative humidity, wind speed, and wind direction) were
119 conducted simultaneously. NO_x and O₃ were analyzed using the Ozone Analyzer (Thermo Fisher Scientific USA,
120 49I) and NO-NO₂-NO_x Analyzer (Thermo Fisher Scientific USA, 17I), respectively. The mass concentration of

121 PM_{2.5} was measured using an oscillating balance analyzer (TH-2000Z, China) (Wang et al., 2014a). The quality
122 assurance of NO₂, O₃, and PM_{2.5} was conducted based on HJ 630-2011 specifications. Meteorological including
123 wind speed (WS), wind direction (WD), relative humidity (RH), air pressure, temperature, ~~air pressure,~~ and
124 precipitation were measured by an automatic weather monitoring system. The planetary boundary height was
125 obtained from the European Centre for Medium-Range Weather Forecasts
126 (<https://www.ecmwf.int/en/forecasts/datasets/browse-reanalysis-datasets>).

127 **2.2 Ozone formation potential (OFP) and secondary formation potential (SOAFP) calculation**

128 The formation potential of O₃ and SOA was used to characterize the relative importance of VOCs species and
129 sources in secondary formation, which were estimated using Eqs. (1) and (2).

$$130 \quad OFP = \sum_i^n MIR_i \times [VOC(ppb)]_i \quad (1)$$

$$131 \quad SOAFP = \sum_i^n Y_i \times [VOC(ppb)]_i \quad (2)$$

132 where n represents the number of VOCs, $[VOC]_i$ represents the i th VOC species concentration, MIR_i is the
133 maximum incremental reactivity for the i th VOC species, and Y_i is the SOA yield of VOC_i (McDonald et al.,
134 2018). The MIR for each VOC species were taken from the updated Carter research results
135 (<http://www.engr.ucr.edu/~carter/reactdat.htm>, last access: 24 February 2021). For species lacking yield curves,
136 the fractional aerosol coefficient (FAC) values proposed by Grosjean and Seinfeld (1989) were used.

137 **2.3 Deweathered model**

138 In this work, ~~a random forest (RF) model was used to assess the meteorology associated variations~~ the influences
139 of meteorological conditions on and quantify the impacts of precursor emissions to O₃ and PM_{2.5} levelswere
140 removed using the random forest (RF) model. The meteorological predictors in the RF model include wind speed
141 (WS), wind direction (WD), air temperature (T), relative humidity (RH), precipitation (Prec), air pressure (P),

142 time predictors (year, day of year (*DOY*), hour) and planetary boundary layer height (*BLH*). These meteorological
143 parameters have been reported to be strongly associated with $PM_{2.5}$ and O_3 concentrations in various regions in
144 China (Chen et al., 2020; Feng et al., 2020) and contributed significantly in previous $PM_{2.5}$ and O_3 prediction
145 models (She et al., 2020; Li et al., 2020). The original dataset was randomly classified into a training dataset (90 %
146 of input dataset) for developing the RF model, and the remaining one was treated as the test dataset. After the
147 building of the RF model, the deweathered technique was applied to predict the air pollutant level at a specific
148 time point. The differences in original pollutant concentrations and deweathered pollutant concentrations were
149 regarded as the concentrations contributed by meteorology. Statistical indicators including R^2 , RMSE, and MAE
150 values were regarded as the major criteria to evaluate the modeling performance.

151 **2.4 Positive matrix factorization (PMF)**

152 In this study, the US EPA PMF 5.0 software was used for VOCs source apportionment (Abeleira et al., 2017; Li
153 et al., 2019a; Xue et al., 2017). The detailed description of the PMF model is found elsewhere (Ling et al., 2011;
154 Yuan et al., 2009). PMF uses both concentration and user-provided uncertainty associated with the data to weight
155 individual points. Species with high percentages of missing values (> 40 %) and with signal-to-noise ratio of
156 below 2 were excluded. Based on this, 53 VOC species including source tracers (e.g., chloromethane,
157 trichloroethylene, tetrachloroethylene and MTBE) and SO_2 were chosen for the source apportionment analysis.
158 Data values below the MDL were replaced by MDL/2, and the missing data were substituted with median
159 concentrations. If the concentration is less than or equal to the MDL provided, the uncertainty is calculated using
160 the equation of $Unc = 5/6 \times MDL$; if the concentration is greater than the MDL provided, the uncertainty is
161 calculated as $Unc = [(error\ factor \times mixing\ ratio)^2 + (MDL)^2]^{1/2}$.

162 During the PMF analysis, the bootstraps (BS) method, displacement (DISP) analysis, and the combination

163 of the DISP and BS (BS-DISP) were used to evaluate the uncertainty of the base run solution. A total of 100
 164 bootstrap runs were performed, and acceptable results were gained for all factors (above 90%). Based on the
 165 DISP analysis, the observed drop in the Q value was below 0.1 %, and no factor swap occurred, confirming that
 166 the solution was stable. The BS-DISP analysis showed that the observed drop in the Q value was less than 0.5 %,
 167 demonstrating that the solution was useful.

168 **2.5 Cluster and potential source contribution function (PSCF) analysis**

169 ~~The potential source contribution function (PSCF) model has been widely used to identify potential source~~
 170 ~~regions of air pollutants (Hong et al., 2019; Liu et al., 2016b, 2019, 2020a; Zheng et al., 2018;). In this study, the~~
 171 ~~24 h backward trajectories (1 h intervals) of air masses arriving at the sampling site with a trajectory height of~~
 172 ~~1500 m were calculated using the MeteoInfoMap software. The study area covered by back trajectories was~~
 173 ~~divided into $0.5^\circ \times 0.5^\circ$ grid cells. The pollution trajectory was defined as the trajectories corresponding to the~~
 174 ~~total VOC (TVOC) concentration that exceeded the 75th percentile concentration of TVOC. PSCF value in the~~
 175 ~~ij th grid was defined as:~~

$$176 \quad \text{PSCF}_{ij} = \frac{m_{ij}}{n_{ij}} \quad (3)$$

177 ~~where the m_{ij} is the number of polluted trajectories through the grid; n_{ij} is the all trajectories through the grid.~~
 178 ~~The weight function W_{ij} is applied to reveal the uncertainty of small values of n_{ij} (Polissar et al., 1999; Li et al.,~~
 179 ~~2017):~~

$$180 \quad W_{ij} = \begin{cases} 1.00 & 80 < n_{ij} \\ 0.70 & 20 < n_{ij} \leq 80 \\ 0.42 & 10 < n_{ij} \leq 20 \\ 0.05 & n_{ij} \leq 10 \end{cases} \quad (4)$$

181 **3. Results and discussion**

182 3.1 TVOC mixing ratios and chemical composition

183 The time series of meteorological parameters and concentrations of air pollutants during the measurement
184 period are shown in Fig. 1. The ambient temperature ranged from -13.3°C to 38.7°C and the RH varied between
185 5% and 99% across the sampling months. Prevailing winds shifted between southwesterly and northeasterly with
186 WS of 0–6.8 m s⁻¹. The mixing ratio of total VOCs (TVOC) ranged from 5.5–118.7 ppbv during the sampling
187 period with relatively higher values during September and November (49.9-51.6 ppbv) while relatively lower
188 values (22.2-27.5 ppbv) across the other months. Major VOC compositions were generally consistent during the
189 whole measurement period. Alkanes, OVOCs and halocarbons were the dominant chemical groups, accounting
190 for 75-81% of the TVOCs across the sampling months. In terms of individual species, acetone, dichloromethane,
191 butane, toluene, methyl tert butyl ether (MTBE), *i*-pentane, propylene, hexane, 1,1- dichloroethane, benzene and
192 1-butene made up the largest contribution, accounting for 50.6 % of the TVOC on average during the whole
193 measurement period.

194 The comparison of concentration and composition of chemical groups observed in this work and previous
195 studies is shown in Fig. 2. Clearly, the concentrations of TVOCs and major VOC groups observed in this study
196 were apparently lower than those in 2014 and 2016 in urban sites in Beijing (An et al., 2012; Liu et al., 2020a;
197 Li et al., 2015b), indicating the effectiveness of control measures in most recent years on lowering VOCs emission.
198 Besides, the composition of major chemical groups also showed remarkable changes, with decreased proportions
199 of alkanes while increased fractions of halocarbons, aromatics and OVOCs, reflecting the changes in emission
200 sources types in most recent years.

201 During the measurement period, ~~nine~~ 14 O₃ ~~pollution days~~ ~~pollution events~~ (~~days with~~ maximum ~~daily~~ 8-h
202 average O₃ exceeding 160 µg m⁻³) were observed, ~~which occurred during~~ (*i.e.*, 17-22 April, 3-17 May, 18-29 June,

203 2-13 July, and 25-29 September of 2019), and April, May, June, July, and September of 2019 were defined as
204 the O₃-polluted months. ~~The months with O₃ pollution events were classified as high O₃ months in this study,~~
205 ~~which were further classified into the clean and polluted days based on the measured concentrations.~~ The
206 comparison of meteorological parameters and trace gases on O₃ pollution and compliance days (days with
207 maximum 8-h average O₃ below 160 μg m⁻³) of ~~During~~ the four high-O₃-polluted months ~~(i.e., April, May, June,~~
208 ~~July, and September)~~ is shown in Fig. 3. ~~the~~ The WS on O₃ pollution ~~polluted~~ days ($1.31 \pm 0.90 \text{ m s}^{-1}$) was
209 slightly lower than that on O₃ compliance ~~clean~~ days ($1.47 \pm 1.10 \text{ m s}^{-1}$), indicating that precursors were more
210 conducive to be diluted on O₃ compliance ~~clean~~ days. The variation trend of O₃ and temperature displayed the
211 negative correlation, and the linear correlations between O₃ and temperature on O₃ pollution ~~polluted~~ days ($R^2 = 0.63$)
212 was stronger than that on O₃ compliance ~~clean~~ days ($R^2 = 0.35$). The mean TVOC concentration ~~higher~~ on O₃
213 pollution days (32.3 ppbv) was higher than that on O₃ compliance ~~clean~~ days (29.6 ppbv), which was mainly
214 ~~contributed by~~ attributed to higher concentrations of MTBE, acrolein, trans-2-butene ~~was higher~~ on pollution ~~polluted~~
215 days. MTBE is widely used as a fuel additive in motor gasoline (Liang et al., 2020), and trans-2-butene is the
216 main component of oil/gas evaporation (Li et al., 2019a). Such result ~~indicated~~ suggested enhanced contribution
217 of traffic emissions on O₃ pollution ~~polluted~~ days. Besides, the concentration of isoprene, which is primarily produced
218 by vegetation through photosynthesis, increased significantly ~~during the~~ on O₃ pollution ~~polluted~~ days probably due to the
219 stronger plant emission at elevated temperature (Guenther et al., 1993, 2012; Stavrou et al., 2014). The ratio
220 of *m/p*-xylene to ethylbenzene (X/E) measured can be used as an indicator of the photochemical aging of air
221 masses because of their similar sources in urban environments and differences in atmospheric lifetimes (Carter,
222 2010; Miller et al., 2012; Wang et al., 2013a). The mean X/E value on O₃ compliance ~~clean~~ days (1.41) was

223 higher than that on O₃ pollution polluted days (1.17), indicating enhanced secondary transformation of VOCs to
224 O₃ during the on O₃ pollutioned periodsdays.

225 The daily PM_{2.5} concentrations ranged from 9-260 µg m⁻³ with the mean value of 88.5 µg m⁻³ during the
226 measurement period. ~~Fourteen-15~~ PM_{2.5} pollution dayevents (daily average PM_{2.5} exceeding 75 µg m⁻³) were
227 observed, ~~which occurred on (i.e.,~~ 1-2 December and 5 December of 2018, 3 January, 12-13 January, 22-23 April,
228 29 April, 12 May, 15 May, 19 October, and 21-23 November of 2019), and December of 2018, January, Apri,
229 May, October and November of 2019 were identified as the PM_{2.5}-polluted months. ~~The months with PM_{2.5}~~
230 ~~pollution events were classified as high PM_{2.5} months, which were also further classified into the clean and~~
231 ~~polluted days based on the measured concentrations. During the six PM_{2.5}-polluted months, T, the WS on PM_{2.5}~~
232 pollution polluted days (1.05 ± 1.06 m s⁻¹) was lower than that on PM_{2.5} compliance clean days (1.43 ± 1.06 m s⁻
233 ¹), indicating the weaker ability of winds for the dilution and diffusion of precursor on PM_{2.5} pollutioned days.
234 Both the value of relative humidity (RH) and TVOCs increased significantly on PM_{2.5} pollution polluted days,
235 suggesting that the secondary transformation of VOCs was more conducive at higher RH. The mean X/E value
236 on PM_{2.5} compliance clean days (1.47) was slightly higher than that on PM_{2.5} pollution polluted days (1.44),
237 indicating enhanced secondary transformation of VOCs ~~to PM_{2.5} during the on PM_{2.5} pollution periodsdays~~.

238 **3.2 The role of VOCs on secondary pollution**

239 **3.2.1 Estimating O₃ and PM_{2.5} levels contributed by emissions**

240 O₃ and secondary aerosols are primarily formed via photochemical reactions in the atmosphere, of which
241 concentrations could be largely influenced by meteorological conditions (Chen et al., 2020; Feng et al., 2020;
242 Zhai et al., 2019). In this work, the respective contributions of meteorology and emissions to PM_{2.5} and O₃
243 variations were determined using the RF model as described in section 2.3. The coefficients of determination (R^2)

244 for the RF model in predicting PM_{2.5} and O₃ are 0.85 and 0.91, respectively (Shown in Fig. S2). The respective
245 contributions of anthropogenic and meteorology to O₃ and PM_{2.5} during each period is shown in Fig. 4. During
246 the ~~high-O₃-polluted~~ months, the meteorologically-driven O₃ level on ~~the O₃ pollution~~ ~~polluted~~ days (72.5 μg m⁻³)
247 ³⁾ was significantly higher than that on ~~the clean~~O₃ compliance days (35.3 μg m⁻³). After removing the
248 meteorological contribution, the residual emission-driven O₃ level on ~~O₃ pollutioned~~ ~~days~~ (45.3 μg m⁻³) and
249 compliance clean days (44.9 μg m⁻³) of the ~~high-O₃-polluted~~ months was almost identical and were significantly
250 higher than that during the ~~lownon-O₃-polluted~~ months (23.8 μg m⁻³). The emission-driven PM_{2.5} level was in
251 the order of: PM_{2.5} pollutioned days of the ~~high-PM_{2.5}-polluted~~ months (55 μg m⁻³) > PM_{2.5} complianceclean
252 days of the ~~high-PM_{2.5}-polluted~~ months (44 μg m⁻³) > ~~lownon-PM_{2.5}-polluted~~ months (29 μg m⁻³). These results
253 suggested that apart from meteorological factors, emissions also play a role in deteriorating PM_{2.5} and O₃
254 pollution, and reducing anthropogenic emissions is essential for improving air quality.

255 The VOCs/NO_x ratio has been widely used to distinguish whether the O₃ formation is VOC limited or NO_x
256 limited (Li et al., 2019a). Generally, VOC-sensitive regime occurs when VOCs/NO_x ratios are below 10 while
257 NO_x-sensitive regime occurs when VOCs/NO_x ratios are higher than 20 (Hanna et al., 1996; Sillman, 1999). In
258 this study, the values of VOCs/NO_x (ppbv ppbv⁻¹) were all below 3 during both the O₃-polluted and ~~lownon-O₃-~~
259 polluted months (Fig. S3), suggesting that the O₃ formation was sensitive to VOCs, and thus the reductions of
260 the emissions of VOCs will be beneficial for O₃ alleviation.

261 **3.2.2 Contribution of VOCs to OFP and SOAFP**

262 As discussed in 3.1, O₃ formation was generally VOCs-sensitive during the measurement period.
263 Quantifying the contribution of speciated VOCs species to O₃ is helpful for developing effective VOCs control
264 measures and alleviating O₃ pollution. The averaged OFP on O₃ pollution days of the O₃-polluted months, O₃

265 compliance days of the O₃-polluted months, and during the non-O₃-polluted months were 224.9, 201.4, and 187.5
266 $\mu\text{g m}^{-3}$, respectively (Fig. 5). According to our observations, the higher OFP on O₃ polluted days than that on
267 O₃ compliance clean days of during the O₃-polluted months was mainly contributed by attributed to higher levels
268 of trans-2-butene, o-xylene and acrolein O₃ on polluted days, in line with that in Fig. 3. Alkenes, aromatics
269 and OVOCs were the three biggest contributors contributing chemical groups to O₃ formation, accounting for
270 85.1%, 85.7% and 81.6% of the total OFP on O₃ pollution days of the O₃-polluted months, O₃ compliance days
271 of the O₃-polluted months, and during the non-O₃-polluted months, respectively. In terms of the individual
272 species, the top 10 highest contributors during the high-O₃-polluted months were toluene (7.5% and 6.4% on O₃
273 clean compliance and polluted days, respectively), trans-2-butene (7.5% and 9.6%), acrolein (5.7% and 10.8%),
274 m/p-xylene (6.9% and 6.1%), o-xylene (5.8% and 6.6%), 1-butene (7.1% and 5.2%), 1-hexene (5.4% and 4.4%),
275 vinyl acetate (5.7% and 4.2%), methyl methacrylate (4.8% and 5.5%), and 1-pentene (4.4% and 4.5%). During
276 the low non-O₃-polluted months, the overall OFP was mainly contributed by toluene (10.8%), trans-2-butene
277 (10.5%), 1-butene (7.3%), m/p-xylene (6.5%), 1-pentene (5.7%), 1-hexene (5.0%), methyl methacrylate (4.9%),
278 o-xylene (4.9%), vinyl acetate (3.8%), and isopentane (2.3%), respectively.

279 As shown in Fig. S3, the ratio of VOCs/NO_x was generally below 3 during the sampling period, indicating
280 high NO_x conditions. Based on the estimated yields of the VOCs shown in Table S1S2, the SOAFPs were
281 calculated and compared in Fig. 5. The mean SOAFP on PM_{2.5} pollution days of the PM_{2.5}-polluted months,
282 PM_{2.5} compliance days of the PM_{2.5}-polluted months, and during the non-PM_{2.5}-polluted months were 1.28, 1.07,
283 and 0.89 $\mu\text{g m}^{-3}$, respectively. During the six PM_{2.5}-polluted months, The higher SOAFP on PM_{2.5} polluted
284 pollution days of the high-PM_{2.5} months than that on PM_{2.5} compliance clean days of the PM_{2.5} months was
285 mainly contributed by attributed to higher levels of 1,2,4-trimethylbenzene, n-undecanone, n-Nonane, 1,4-

286 diethylbenzene, and 1,3-diethylbenzene on PM_{2.5} polluted days. Aromatics have the largest SOAFP,
287 accounting for 74% and 75% of the total SOAFP on PM_{2.5} pollution and compliance clean days of the high-
288 PM_{2.5}-polluted months, and 70% of the total SOAFP~~polluted days of the high PM_{2.5} months and~~ during the
289 ~~lownon-~~PM_{2.5}-polluted months, respectively. The 10 species responsible for most of the SOAFP were toluene
290 (41% and 40% on PM_{2.5} pollution and compliance days ~~polluted days~~ of the high-PM_{2.5}-polluted months, ~~40%~~
291 ~~on clean days of the high-PM_{2.5} months,~~ and 33% during the ~~lownon-~~PM_{2.5}-polluted months), 1-hexene (13.0%,
292 12.5%, and 15.2%), xylenes (11.6%, 14.1% and 14.8%), ethylbenzene (4.9%, 5.3% and 6.0%), styrene (4.5%,
293 5.6% and 5.6%), 1-pentene (3.3%, 3.4% and 4.3%), methyl cyclopentane (2.1%, 2.7% and 3.6%), 1,2,3-
294 trimethylbenzene (2.8%, 2.4% and 2.8%), m-ethyl toluene (1.7%, 1.4% and 1.7%) and p-ethyl toluene (1.7%,
295 1.4% and 1.7%), respectively.

296 **3.3 Source apportionment of VOCs**

297 **3.3.1 Indication from tracers**

298 The great changes in the mixing ratios of VOCs species are mainly affected by the photochemical processing
299 and the emission inputs, and ambient ratios for VOCs species having similar atmospheric lifetimes are indicators
300 of different sources (Li et al., 2019a; Raysoni et al., 2017 Song et al., 2021). The ratio of *i*-pentane to *n*-pentane
301 are widely used to examine the impact of vehicle emissions, fuel evaporation and combustion emissions, within
302 the *i/n*-pentane ratios of ranging between 2.2–3.8, 1.8–4.6 and 0.56-0.80, respectively (McGaughey et al., 2004;
303 Jobson et al., 2004; Russo et al., 2010; Wang et al., 2013b; Yan et al., 2017). As shown in Fig. 6, the *i/n*-pentane
304 ratios during the PM_{2.5}-polluted months were mostly within the range of 0.3-2.0, suggesting the pentanes were
305 from the mixed sources of coal combustion and fuel evaporation. During the non-PM_{2.5}-polluted months, the *i/n*-
306 pentane ratios were distributed in the range of 1.3-3.4, indicating strong impacts from vehicle exhaust and fuel

307 evaporation. During the O₃-polluted months, most of the i/n-pentane ratios (1.5-2.5) were distributed within the
308 reference range of vehicle exhaust and fuel evaporation, whereas most of the i/n-pentane ratios during the non-
309 O₃-polluted months ranged between 1.7-2.1, suggesting the significant impact of fuel evaporation.

310 The toluene/benzene (T/B) ratio, a widely used indicator for sources of aromatics. In areas heavily impacted
311 by vehicle emissions, the T/B ratio lies in the range of 0.9–2.2 (Qiao et al., 2012; Dai et al., 2013; Wang et al.,
312 2013c; Yao et al., 2013; Zhang et al., 2013; Yao et al., 2015a; Mo et al., 2016; Deng et al., 2018). Higher T/B
313 ratios were reported for solvent use (greater than 8.8) (Yuan et al., 2010; Wang et al., 2014b; Zheng et al., 2013)
314 and industrial processes (1.4-5.8) (Mo et al., 2015; Shi et al., 2015). In burning source emission studies, the T/B
315 ratio was below 0.6 in different combustion process and raw materials (Tsai et al., 2003; Akagi et al., 2011; Mo
316 et al., 2016). Most of the T/B ratios during the PM_{2.5}-polluted and non-PM_{2.5}-polluted months were within the
317 range of 1.1-1.8 and 0.8-2.2, whereas the T/B ratios were mostly distributed within the range of 0.8-2.2 and 0.9-
318 1.9 during the O₃-polluted and non-O₃-polluted months, respectively, suggesting the significant impact of vehicle
319 and industrial emissions.

320 **3.3.2 PMF**

321 The factor profiles given by PMF and the contribution of each source to ambient VOCs during each period
322 is presented in Fig. 76 and Fig. 78, respectively. Six emission sources were identified: coal/biomass burning,
323 solvent use, industrial sources, oil gas evaporation, gasoline vehicle emission, and diesel vehicle emission based
324 on the corresponding markers for each source category. In general, diesel vehicle exhaust, gasoline vehicle
325 exhaust and industrial emissions were the main VOCs sources during both the O₃-polluted and PM_{2.5}-polluted
326 months, with total contributions of 62% and, 62% on O₃ pollution and compliance days of the O₃-polluted months,
327 and 66% and 59% on PM_{2.5} pollution and compliance days of the PM_{2.5}-polluted months, respectively. ~~Diesel~~

328 ~~and gasoline vehicle exhaust exhibited obvious higher contributions while combustion and industrial sources~~
329 ~~showed lower contributions during the high O₃ months than that during the low O₃ months. The O₃-polluted~~
330 ~~months exhibited higher proportions of diesel (24% on O₃ compliance days and 27% on O₃ pollution days) and~~
331 ~~gasoline vehicle emission (17% on O₃ compliance days and 16% on O₃ pollution days) compared with the non-~~
332 ~~O₃-polluted months (8% and 13%, respectively). During the O₃-polluted months, the contributions of industrial~~
333 ~~emissions (22%) and fuel evaporation (18%) on O₃ polluted days were much higher than those on O₃~~
334 ~~compliance clean days (18% and 13%, respectively). Figure 9 presents the relative contributions of individual~~
335 ~~VOC sources from PMF to OFP. On the base of O₃ formation impact, diesel and gasoline vehicle exhaust were~~
336 ~~major contributors. During the O₃-polluted months, vehicle emissions and fuel evaporation showed higher OFP~~
337 ~~values on O₃ pollution days (93.9 and 35.5 μg m⁻³) was higher compared with those on O₃ compliance days (88.0~~
338 ~~μg m⁻³ and 25.8 μg m⁻³, respectively). Besides, fuel evaporation also showed higher OFP (35.5 μg m⁻³) and served~~
339 ~~as an important contributor (18%) for O₃ formation on O₃-polluted days. Although industrial emissions act as an~~
340 ~~important source for VOCs concentrations on O₃-polluted days (shown in Fig. 8), the potential to form O₃ is~~
341 ~~limited, accounting for 11% of the total OFP. As illustrated shown in Fig. 7, the industrial source was distinguished~~
342 ~~by high compositions of alkanes while relatively lower compositions of alkenes and aromatics, resulting in low~~
343 ~~O₃ formation potentials. Such results suggested that the fuel use and diesel vehicle exhaust should be controlled~~
344 ~~preferentially for O₃ mitigation.~~

345 The PM_{2.5}-polluted months showed higher proportions of industrial (29% on both PM_{2.5} compliance and
346 PM_{2.5} pollution days) and coal/biomass combustion emissions (16% on PM_{2.5} compliance days and 18% on PM_{2.5}
347 pollution days) compared with the non-PM_{2.5}-polluted months (17% and 10%, respectively). The PM_{2.5} pollution
348 days were dominated by industrial emission (29%), diesel vehicle exhaust (24%), and combustion source (18%).

349 During the PM_{2.5}-polluted months, the contribution of diesel vehicle exhaust on PM_{2.5} pollution days (24%-) was
350 ~~much~~ higher than ~~those that~~ on PM_{2.5} compliance days (~~4816~~%). On the base of PM_{2.5} formation impact, diesel
351 vehicle exhaust and combustion were two major contributors on PM_{2.5} pollution days (shown in Fig. 9), and these
352 two sources showed obvious higher SOAFP on PM_{2.5} pollution days (0.30 and 0.32 $\mu\text{g m}^{-3}$, respectively) ~~than~~
353 ~~that compared with those~~ on PM_{2.5} compliance days of the PM_{2.5}-polluted months (0.15 and 0.14 $\mu\text{g m}^{-3}$,
354 respectively). Although industrial emissions act as an important source for VOCs concentrations on PM_{2.5}-
355 pollution days, the potential to form PM_{2.5} is limited, accounting for 16% of the total SOAFP. The above results
356 suggested that diesel vehicle exhaust and combustion should be controlled preferentially for alleviating PM_{2.5}
357 pollution.

358 Based on the mass concentrations of individual species in each source, m/p-xylene, o-xylene, methyl
359 methacrylate, vinyl acetate, 1-hexene, and acrolein in gasoline and diesel vehicular emissions; toluene, trans-2-
360 butene, and 1-pentene in fuel evaporation and diesel vehicular emissions; acrolein in solvent, gasoline vehicular
361 and diesel vehicular emissions were the dominant species contributing to photochemical O₃ formation (Fig. 109).
362 Toluene, m/p-xylene, o-xylene, styrene, ethylbenzene, 1-pentene, 1,2,3-trimethylbenzene from combustion and
363 diesel vehicular emissions; 1-hexene from diesel vehicular emission; and methyl cyclopentane from combustion,
364 industrial and diesel vehicular emissions were the dominant contributors for SOA formation during the PM_{2.5}
365 pollution periods (Fig. 109).

366 **3.4 Influence of source regions**

367 ~~Regional transport is an essential source for VOCs in addition to local emissions. The possible geographic origins~~
368 ~~of the VOC sources were explored using PSCF as shown in Fig. 10 and 11. Diversities of geographic origins~~
369 ~~were found for different periods. During the high O₃ months, high PSCF values were found in Beijing and the~~

370 junction of Hebei province while the PSCF showed high values in Inner Mongolia, northern Shanxi, Hebei, and
371 Beijing during the clean months. The air mass backward trajectory cluster analysis indicated that the VOCs
372 concentration was significantly affected by pollution transmission at the Shanxi Province and Hebei Province
373 junction and local source emissions during the high O_3 months. Note that the west short distance trajectories
374 (cluster 1 in Fig. 10a) that passed over Shanxi and Hebei provinces exhibited relatively high VOCs concentrations
375 and OFP, mainly contributed by aromatics. In addition, although the VOCs concentration of the trajectories from
376 the south (cluster 3 in Fig. 10) was relatively small, the OFP in these pollution trajectories were the highest due
377 to relatively higher proportion of aromatics. Therefore, in addition to local emissions, the transmission of highly
378 polluting air masses from the western and southern Hebei should be paid attention for controlling emissions of
379 reactive VOCs compounds. During the low O_3 months, the VOCs concentration was mainly affected by the
380 northwest trajectory that originate from Inner Mongolia and passed through the western Hebei, reflecting large-
381 scale and long distance transport of VOCs. Besides, the air masses from the southern region (cluster 1 in Fig.
382 10c), representing pollution transmission from Shanxi and Hebei provinces also have significant impact on VOCs
383 concentration. Note that the VOCs concentration during the O_3 -clean months were relatively higher compared
384 with those during the polluted months. Fast moving air masses from the northwest Inner Mongolia typically carry
385 clean air masses (Zhang et al., 2017b). It is proposed that the higher VOCs concentration during the low O_3
386 months was related to domestic coal/biomass burning in the northern regions during cold seasons. However, the
387 OFP during the low O_3 months were generally lower than those during pollution months, ascribing to lower
388 contributions of OVOCs.

389 The VOCs concentration was mainly affected by local emissions on $PM_{2.5}$ -polluted days according to the
390 PSCF result. Besides, the air masses that originated from Inner and passed through western Hebei also played an

391 important role in affecting the VOCs concentration as indicated by the relatively high VOCs concentration and
392 SOAFP for this trajectory cluster. The south trajectories originating from the junction of Hebei province exhibited
393 relatively low VOCs concentration. However, the SOAFP of this trajectory cluster was relatively high because
394 of high proportion. Specifically, the proportion of southwest trajectories with high density emissions to the total
395 trajectories was higher on PM_{2.5} pollution days (65.6%) than that on clean days (25.3%). During the low PM_{2.5}
396 months, the VOCs concentration was mainly affected by the short distance northern (42.9%, cluster 2 in Fig. 11c)
397 and western trajectories (29.8%, cluster 1 in Fig. 11c). Although the proportion of the southern trajectories
398 (cluster 4 in Fig. 11c) to the total trajectories was relatively lower, both the VOCs concentration and the SOAFP
399 of this trajectory cluster was the highest. Overall, the above results indicated that the transmission of highly
400 polluting air masses from the junction of western and southern Hebei province should be paid attention for
401 controlling emissions of reactive VOCs compounds and alleviating PM_{2.5} pollution.

402 4. Conclusions

403 In this work, the field sampling campaign of VOCs was conducted at urban Beijing during December 2018 and
404 November 2019 ~~to investigate the characteristics, sources and secondary transformation potential the role of~~
405 ~~VOCs at an urban site in Beijing. In total, 95 VOCs including 25 alkanes, 8 alkenes, 16 aromatics, 34 halocarbons~~
406 ~~and 12 OVOC were identified and quantified.~~ The VOCs concentrations ranged from 5.5 to 118.7 ppbv with
407 mean value of 34.9 ppbv. ~~In terms of the composition, a~~ Alkanes, OVOCs and halocarbons were the dominant
408 chemical groups, accounting for 75-81% of the TVOCs across the sampling months. Nine 14 O₃ pollution events
409 and fourteen 15 PM_{2.5} pollution events days were observed during the sampling period. By excluding the
410 meteorological impact, the ~~O₃ level driven by~~ emission drives O₃ level during the O₃-polluted months were
411 higher than that during the non-O₃-cleanpolluted months, and similar pattern was found for PM_{2.5}. The molar

412 ratio of VOCs to NO_x indicated that O₃ formation was limited by VOCs during both the O₃-polluted ~~and O₃-~~
413 ~~clean-non-O₃-polluted~~ months, and thus reducing VOCs emission is essential for alleviation of O₃ pollution. The
414 contributions of coal/biomass combustion, solvent use, industrial sources, oil/gas evaporation, gasoline exhaust,
415 and diesel exhaust were identified based on PMF analysis. ~~By e~~Considering both the concentration and maximum
416 incremental reactivity of individual VOC species for each source, fuel use and diesel exhaust sources were
417 identified as the main contributors of O₃ formation during the O₃-polluted months, particularly the VOCs species
418 of toluene, xylenes, trans-2-butene, acrolein, methyl methacrylate, vinyl acetate, 1-butene and 1-hexene ~~were~~
419 ~~identified as the main contributors of O₃ formation during the O₃-polluted months,~~ illustrating the necessity of
420 conducting emission controls on these pollution sources and species for alleviating O₃ pollution. VOCs from
421 diesel vehicles and combustion were found to be the dominant contributors for SOAFP, particularly the VOC
422 species of toluene, 1-hexene, xylenes, ethylbenzene and styrene, and top priority should be given to these for the
423 alleviation of haze pollution. ~~The PSCF analysis showed that O₃ and PM_{2.5} pollution was mainly affected by local~~
424 ~~emissions. Besides, the transmission of highly polluting air masses from the western and southern Hebei should~~
425 ~~also be paid attention for O₃ and PM_{2.5} pollution control.~~

426 Acknowledgements

427 This work was supported by the National Natural Science Foundation of China ([9204430221625704](#)) and
428 the Beijing Municipal Science and Technology Project ([Z211100004321006](#) & [Z191100009119001](#) &
429 [Z181100005418018](#)).

430 Data availability

431 The meteorological data are available at <http://data.cma.cn/> (China Meteorological Administration). The
432 website can be browsed in English <http://data.cma.cn/en>. The concentrations of air pollutants including PM_{2.5},

- 433 O₃ and NO_x are available at <https://air.cnemc.cn:18007/> (Ministry of Ecology and Environment the People's
- 434 Republic of China). The website can be browsed in English <http://english.mee.gov.cn/>.

435 **References**

- 436 Abeleira, A., Pollack, I. B., Sive, B., Zhou, Y., Fischer, E. V., Farmer, D. K., 2017. Source characterization of
437 volatile organic compounds in the Colorado Northern Front Range Metropolitan Area during spring and summer
438 2015, *J. Geophys. Res.-Atmos.*, 122, 3595–3613, <https://doi.org/10.1002/2016jd026227>.
- 439 Ahmad, W., Coeur, C., Tomas, A., Fagniez, T., Brubach, J. B., Cuisset, A., 2017. Infrared spectroscopy of
440 secondary organic aerosol precursors and investigation of the hygroscopicity of SOA formed from the OH
441 reaction with guaiacol and syringol. *Appl. Opt.* 56, E116, <https://doi.org/10.1364/AO.56.00E116>.
- 442 [Akagi, S. K., Yokelson, R. J., Wiedinmyer, C., Alvarado, M. J., Reid, J. S., Karl, T., Crouse, J. D., Wennberg,](#)
443 [P. O., 2011. Emission factors for open and domestic biomass burning for use in atmospheric models. *Atmos.*](#)
444 [*Chem. Phys.* 11, 4039–4072.](#)
- 445 Atkinson, R., 2000. Atmospheric chemistry of VOCs and NO_x. *Atmos. Environ.* 34, 2063–2101,
446 [https://doi.org/10.1016/S1352-2310\(99\)00460-4](https://doi.org/10.1016/S1352-2310(99)00460-4).
- 447 An, J.L., Wang, Y.S., Wu, F.K., Zhu, B., 2012. Characterizations of volatile organic compounds during high
448 ozone episodes in Beijing, China. *Environ. Monit. Assess.* 184, 1879e1889.
- 449 Carter, W.P.L. and Atkinson, R., 1989. Computer modeling study of incremental hydrocarbon reactivity. *Environ.*
450 *Sci. Technol.* 23, 864–880, <https://doi.org/10.1021/es00065a017>.
- 451 Carter, W.P.L., 2010. Development of the SAPRC-07 chemical mechanism, *Atmos. Environ.* 44, 5324–5335,
452 <https://doi.org/10.1016/j.atmosenv.2010.01.026>.
- 453 Chang, T.Y. and Rudy, S.J., 1990. Ozone-forming potential of organic emissions from alternative-fueled vehicles,
454 *Atmos. Environ.*, 24, 2421–2430, [https://doi.org/10.1016/0960-1686\(90\)90335-K](https://doi.org/10.1016/0960-1686(90)90335-K).

455 Chen, L., Zhu, J., Liao, H., Yang, Y., Yue, X., 2020. Meteorological influences on PM_{2.5} and O₃ trends and
456 associated health burden since China's clean air actions, *Sci. Total Environ.* 744, 140837,
457 <https://doi.org/10.1016/j.scitotenv.2020.140837>.

458 [Dai, P., Ge, Y., Lin, Y., Su, S., and Liang, B., 2013. Investigation on characteristics of exhaust and evaporative](#)
459 [emissions from passenger cars fueled with gasoline/methanol blends. *Fuel.* 113, 10–16.](#)

460 [Deng, C. X., Jin, Y. J., Zhang, M., Liu, X. W., Yu, Z.M., 2018. Emission Characteristics of VOCs from On-Road](#)
461 [Vehicles in an Urban Tunnel in Eastern China and Predictions for 2017–2026. *Aerosol Air Qual. Res.* 18, 3025–](#)
462 [3034.](#)

463 [Doumbia, T., Granier, C., Elguindi, N., Bouarar, I., Darras, S., Brasseur, G., Gaubert, B., Liu, Y., Shi, X.,](#)
464 [Stavrou, T., Tilmes, S., Lacey, F., Deroubaix, A., Wang, T., 2021. Changes in global air pollutant emissions](#)
465 [during the COVID-19 pandemic: a dataset for atmospheric modeling. *Earth Syst. Sci. Data.* 13, 4191–4206.](#)

466 Fan, H., Zhao, C., Yang, Y., 2020. A Comprehensive Analysis of the Spatio-Temporal Variation of Urban Air
467 Pollution in China During 2014–2018, *Atmos. Environ.*, 220, 117066,
468 <https://doi.org/10.1016/j.atmosenv.2019.117066>.

469 Feng, J., Liao, H., Li, Y., Zhang, Z., Tang, Y., 2020. Long-term trends and variations in haze-related weather
470 conditions in north China during 1980–2018 based on emission-weighted stagnation intensity. *Atmos. Environ.*
471 240, 117830, <https://doi.org/10.1016/j.atmosenv.2020.117830>.

472 Fu, Y., Liao, H., Yang, Y., 2019. Interannual and Decadal Changes in Tropospheric Ozone in China and the
473 Associated Chemistry Climate Interactions: A Review, *Adv. Atmos. Sci.* 36, 975–993.

474 [Gani, S., Bhandari, S., Seraj, S., Wang, D. S., Patel, K., Soni, P., Arub, Z., Habib, G., Hildebrandt Ruiz, L., Apte,](#)
475 [J. S., 2019. Submicron aerosol composition in the world's most polluted megacity: the Delhi Aerosol Supersite](#)
476 [study. Atmos. Chem. Phys. 19, 6843–6859.](#)

477 Grosjean, D., and Seinfeld, J. H., 1989. Parameterization of the formation potential of secondary organic aerosols,
478 Atmos. Environ., 23, 1733-1747, 10.1016/0004-6981(89)90058-9.

479 Guenther, A.B., Zimmerman, P.R., Harley, P.C., Monson, R.K., Fall, R., 1993. Isoprene and monoterpene
480 emission rate variability: Model evaluations and sensitivity analyses. J. Geophys. Res. Atmos. 98, 12609–12617,
481 <https://doi.org/10.1029/93JD00527>.

482 [Guo, S., Hu, M., Zamora, M. L., Peng, J., Shang, D., Zheng, J., Du, Z., Wu, Z., Shao, M., Zeng, L., Molina, M.](#)
483 [J., Zhang, R., 2014. Elucidating severe urban haze formation in China, P Natl. Acad. Sci. US, 111, 17373–17378.](#)

484 [Hallquist, M., Wenger, J.C., Baltensperger, U., Rudich, Y., Simpson, D., Claeys, M., et al., 2009. The formation,](#)
485 [properties and impact of secondary organic aerosol: current and emerging issues. Atmos. Chem & Phys. 9 \(14\),](#)
486 [5155–5236.](#)

487 Han, S., Zhao, Q., Zhang, R., Liu, Y., Li, C., Zhang, Y., Li, Y., Yin, S., Yan, Q., 2020. Emission characteristic
488 and environmental impact of process-based VOCs from prebaked anode manufacturing industry in Zhengzhou,
489 China. Atmos. Pollut. Res. 627 11, 67-77, 10.1016/j.apr.2019.09.016.

490 Hanna, S. R., Moore, G. E., Fernau, M., 1996. Evaluation of photochemical grid models (UAM-IV, UAM-V,
491 and the ROM/UAMIV couple) using data from the Lake Michigan Ozone Study (LMOS). Atmos. Environ. 30,
492 3265–3279.

493 Hong, Z., Li, M., Wang, H., Xu, L., Hong, Y., Chen, J., Chen, J., Zhang, H., Zhang, Y., Wu, X., Hu, B., Li, M.,
494 2019. Characteristics of atmospheric volatile organic compounds (VOCs) at a mountainous forest site and two

495 urban sites in the southeast of China. *Sci. Total. Environ.* 657, 1491–1500,
496 <https://doi.org/10.1016/j.scitotenv.2018.12.132>.

497 Huang, R.J., Zhang, Y., Bozzetti, C., Ho, K.F., Cao, J.J., Han, Y., Daellenbach, K. R., Slowik, J. G., Platt, S. M.,
498 Canonaco, F., Zotter, P., Wolf, R., Pieber, S. M., Bruns, E. A., Crippa, M., Ciarelli, G., Piazzalunga, A.,
499 Schwikowski, M., Abbaszade, G., Schnelle-Kreis, J., Zimmermann, R., An, Z., Szidat, S., Baltensperger, U., El
500 Haddad, I., Prevot, A.S.H., 2014. High secondary aerosol contribution to particulate pollution during haze events
501 in China, *Nature*, 514, 218-222, 10.1038/nature13774.

502 [Jobson, B. T., Berkowitz, C. M., Kuster, W. C., Goldan, P. D., Williams, E. J., Fesenfeld, F. C., Apel, E. C., Karl,](#)
503 [T., Lonneman, W. A., Riemer, D., 2004. Hydrocarbon source signatures in Houston, Texas: Influence of the](#)
504 [petrochemical industry. *J. Geophys. Res. Atmos.* 109, D24305, <https://doi.org/10.1029/2004jd004887>.](#)

505 [Kuang, Y., He, Y., Xu, W.Y., Yuan, B., Zhang, G., Ma, Z.Q., Wu, C.H., Wang, C.M., Wang, S.H., Zhang, H.Y.,](#)
506 [Tao, J.C., Ma, N., Su, H., Cheng, Y.F., Shao, M., Sun, Y.L., 2020. *Environ Sci & Technol.* 54 \(7\), 3849-3860.](#)

507 [Li, L., Chen, Y., Zeng, L., Shao, M., Xie, S., Chen, W., Lu, S., Wu, Y., Cao, W., 2014. Biomass burning](#)
508 [contribution to ambient volatile organic compounds \(VOCs\) in the Chengdu–Chongqing Region \(CCR\), China.](#)
509 [Atmos. Environ. 99, 403–410.](#)

510 Li, J., Xie, S.D., Zeng, L.M., Li, L.Y., Li, Y.Q., Wu, R.R., 2015. Characterization of ambient volatile organic
511 compounds and their sources in Beijing, before, during, and after Asia-Pacific Economic Cooperation China
512 2014. *Atmos. Chem. Phys.* 15, 7945–7959

513 Li, G., Bei, N., Cao, J., Wu, J., Long, X., Feng, T., Dai, W., Liu, S., Zhang, Q., Tie, X., 2017^a. Widespread and
514 persistent ozone pollution in eastern China during the non-winter season of 2015: observations and source
515 attributions, *Atmos. Chem. Phys.*, 17, 2759–2774, <https://doi.org/10.5194/acp-17-2759-2017>.

516 [Li, Y. J., Sun, Y., Zhang, Q., Li, X., Li, M., Zhou, Z., Chan, C. K., 2017b. Real-time chemical characterization](#)
517 [of atmospheric particulate matter in China: A review, Atmos. Environ., 158, 270–304.](#)

518 Li, B., Ho, S.S.H., Gong, S., Ni, J., Li, H., Han, L., Yang, Y., Qi, Y., Zhao, D., 2019a. Characterization of VOCs
519 and their related atmospheric processes in a central Chinese city during severe ozone pollution periods. Atmos.
520 Chem & Phys. 19, 617-638.

521 Li, K., Jacob, D.J., Liao, H., Shen, L., Zhang, Q., Bates, K.H., 2019c. Anthropogenic Drivers of 2013–2017
522 Trends in Summer Surface Ozone in China. Proc. Natl. Acad. Sci. 116, 422–427.

523 Li, K., Li, J., Tong, S., Wang, W., Huang, R.-J., Ge, M., 2019d. Characteristics of wintertime VOCs in suburban
524 and urban Beijing: concentrations, emission ratios, and festival effects. Atmos. Chem & Phys. 19, 8021-8036.

525 Li, K., Jacob, D.J., Shen, L., Lu, X., De Smedt, I., Liao, H., 2020. Increases in surface ozone pollution in China
526 from 2013 to 2019: anthropogenic and meteorological influences. Atmos. Chem & Phys. 20, 11423-11433.

527 Liang, Y., Liu, X., Wu, F., Guo, Y., Xiao, H., 2020. The year-round variations of VOC mixing ratios and their
528 sources in Kuytun City (northwestern China), near oilfields. Atmos. Pollut. Res. 11,9
529 DOI:10.1016/j.apr.2020.05.022.

530 Liu, B., Liang, D., Yang, J., Dai, Q., Bi, X., Feng, Y., Yuan, J., Xiao, Z., Zhang, Y., Xu, H., 2016a.
531 Characterization and source apportionment of volatile organic compounds based on 1-year of observational data
532 in Tianjin, China. Environ. Pollut. 218, 757–769, <https://doi.org/10.1016/j.envpol.2016.07.072>.

533 Liu, B. S., Liang, D. N., Yang, J. M., Dai, Q. L., Bi, X. H., Feng, Y. C., Yuan, J., Xiao, Z. M., Zhang, Y. F., and
534 Xu, H., 2019b. Characterization and source apportionment of volatile organic compounds based on 1-year of
535 observational data in Tianjin, China. Environ. Pollut. 218, 757–769;
536 <https://doi.org/10.1016/j.envpol.2016.07.072>.

537 Liu, Y., Wang, H., Jing, S., Gao, Y., Peng, Y., Lou, S., Cheng, T., Tao, S., Li, L., Li, Y., 2019. Characteristics
538 and sources of volatile organic compounds (VOCs) in Shanghai during summer: Implications of regional
539 transport. *Atmospheric Environment* 215, 116902.

540 Liu, Y.F., Song, M.D., Liu, X.G., Zhang, Y.P., Hui, L.R., Kong, L.W., Zhang, Y.Y., Zhang, C., Qu, Y., An, J.L.,
541 Ma, D.P., Tan, Q.W., Feng, M., 2020a. Characterization and sources of volatile organic compounds (VOCs) and
542 their related changes during ozone pollution days in 2016 in Beijing, China. *Environ Pollut.* 257, 113599.

543 Liu, Y.M., Wang, T., 2020b. Worsening urban ozone pollution in China from 2013 to 2017–Part 2: The effects
544 of emission changes and implications for multi-pollutant control. *Atmos. Chem. Phys.* 20, 6323–6337.

545 Liu, C., Shi, K., 2021. A review on methodology in O₃-NO_x-VOC sensitivity study. *Environmental pollution*,
546 118249.

547 Lu, X., Zhang, L., Wang, X., Gao, M., Li, K., Zhang, Y., Yue, X., Zhang, Y., 2020. Rapid increases in warm-
548 season surface ozone and resulting health impact in China since 2013. *Environ. Sci & Technol Lett.* 7, 240-247.

549 McDonald, B.C., de Gouw, J.A., Gilman, J.B., Jathar, S.H., Akherati, A., Cappa, C.D., Jimenez, J.L., Lee-Taylor,
550 J., Hayes, P.L., McKeen, S.A., Cui, Y.Y., Kim, S.W., Gentner, D.R., Isaacman-VanWertz, G., Goldstein, Allen
551 H., Harley, R.A., Frost, G.J., Roberts, J. M., Ryerson, T.B., Trainer, M., 2018. Volatile chemical products
552 emerging as largest petrochemical source of urban organic emissions, *Science*, 359, 760,
553 <https://doi.org/10.1126/science.aaq0524>.

554 [McGaughey, G. R., Desai, N. R., Allen, D. T., Seila, R.L., Lonneman, W. A., Fraser, M. P., Harley, R. A., Pollack,](#)
555 [A. K., Ivy, J. M., Price, J. H., 2004. Analysis of motor vehicle emissions in a Houston tunnel during the TexasAir](#)
556 [Quality Study 2000. *Atmos. Environ.* 38, 3363 – 3372.](#)

557 Miller, L., Xu, X., Grgicak-Mannion, A., Brook, J., Wheeler, A., 2012. Multi-season, multiyear concentrations
558 and correlations amongst the BTEX group of VOCs in an urbanized industrial city. *Atmos. Environ.* 61, 305–
559 315.

560 [Mo, Z., Shao, M., Lu, S., Qu, H., Zhou, M., Sun, J., Gou, B., 2015. Process-specific emission characteristics of](#)
561 [volatile organic compounds \(VOCs\) from petrochemical facilities in the Yangtze River Delta, China. *Sci. Total*](#)
562 [Environ. 533, 422–431.](#)

563 [Mo, Z., Shao, M., Lu, S., 2016. Compilation of a source profile database for hydrocarbon and OVOC emissions](#)
564 [in China. *Atmos. Environ.* 143, 209–217.](#)

565 Odum, J.R., Jungkamp, T.P.W., Griffin, R.J., Flagan, R.C., Seinfeld, J.H., 1997. The atmospheric aerosol-
566 forming potential of whole gasoline vapor. *Science.* 276, 96–99.

567 Peng, J., Hu, M., Shang, D., Wu, Z., Du, Z., Tan, T., Wang, Y., Zhang, F., Zhang, R., 2021. Explosive secondary
568 aerosol formation during severe haze in the North China Plain. *Environ Sci & Technol.* 55, 2189-2207.

569 Polissar, A.V., Hopke, P.K., Paatero, P., Kaufmann, Y.J., Hall, D.K., Bodhaine, B.A., Dutton, E.G., Harris, J.M.,
570 1999. The aerosol at Barrow, Alaska: long-term trends and source locations. *Atmos. Environ.* 33, 2441–2458,
571 [https://doi.org/10.1016/S1352-2310\(98\)00423-3](https://doi.org/10.1016/S1352-2310(98)00423-3), 1999.

572 [Qiao, Y.Z., Wang, H.L., Huang, C., Chen, C.H., Su, L.Y., Zhou, M., Xu, H., Zhang, G.F., Chen, Y.R., Li, L., Chen,](#)
573 [M.H., Huang, H.Y., 2012. Source Profile and Chemical Reactivity of Volatile Organic Compounds from Vehicle](#)
574 [Exhaust. *Huanjing Kexue.* 33, 1071–1079.](#)

575 [Raysoni, A.U., Stock, T.H., Sarnat, J.A., Chavez, M.C., Sarnat, S.E., Montoya, T., Holguin, F., Li, W.W., 2017.](#)
576 [Evaluation of VOC concentrations in indoor and outdoor microenvironments at near-road schools. *Environ.*](#)
577 [Pollut. 231, 681–693.](#)

578 [Roger, A. and Janet, A., 2003. Atmospheric degradation of volatile organic compounds. Chem. Rev. 103, 4605,](#)
579 [https://doi.org/10.1021/cr0206420.](https://doi.org/10.1021/cr0206420)

580 [Russo, R. S., Zhou, Y., White, M. L., Mao, H., Talbot, R., Sive, B. C., 2010. Multi-year \(2004–2008\) record of](#)
581 [nonmethane hydrocarbons and halocarbons in New England: seasonal variations and regional sources. Atmos.](#)
582 [Chem. Phys. 10, 4909–4929.](#)

583 Sato, K., Takami, A., Isozaki, T., Hikida, T., Shimono, A., Imamura, T., 2010. Mass spectrometric study of
584 secondary organic aerosol formed from the photo-oxidation of aromatic hydrocarbons. Atmos. Environ. 44,
585 1080–1087, <https://doi.org/10.1016/j.atmosenv.2009.12.013>.

586 Shao, M., Zhang, Y., Zeng, L., Tang, X., Zhang, J., Zhong, L., Wang, B., 2009. Ground-level ozone in the Pearl
587 River Delta and the roles of VOC and NO_x in its production. J. Environ. Manage. 90, 512-518.

588 She, Q., Choi, M., Belle, J. H., Xiao, Q., Bi, J., Huang, K., Meng, X., Geng, G., Kim, J., He, K., Liu, M., Liu, Y.,
589 2020. Satellite-based estimation of hourly PM_{2.5} levels during heavy winter pollution episodes in the Yangtze
590 River Delta, China. Chemosphere. 239, 124678, <https://doi.org/10.1016/j.chemosphere.2019.124678>.

591 Shen, L., Jacob, D. J., Liu, X., Huang, G., Li, K., Liao, H., Wang, T., 2019. An evaluation of the ability of the
592 Ozone Monitoring Instrument (OMI) to observe boundary layer ozone pollution across China: application to
593 2005–2017 ozone trends. Atmos. Chem. Phys. 19, 6551–6560, <https://doi.org/10.5194/acp-19-6551-2019>.

594 Shen, L., Wang, Z., Cheng, H., Liang, S., Xiang, P., Hu, K., Yin, T., Yu, J., 2020. A Spatial-Temporal Resolved
595 Validation of Source Apportionment by Measurements of Ambient VOCs in Central China, Int. J. Env. Res. Pub.
596 He. 17, 791, <https://doi.org/10.3390/ijerph17030791>.

597 [Shi, J., Deng, H., Bai, Z., Kong, S., Wang, X., Hao, J., Han, X., Ning, P., 2015. Emission and profile characteristic](#)
598 [of volatile organic compounds emitted from coke production, iron smelt, heating station and power plant in](#)
599 [Liaoning Province, China. Sci. Total Environ. 515, 101–108.](#)

600 Sillman, S., 1999. The relation between ozone, NO_x and hydrocarbons in urban and polluted rural environments,
601 Atmos. Environ., 33, 1821–1845, 1999.

602 [Sindelarova, K., Markova, J., Simpson, D., Huszar, P., Karlicky, J., Darras, S., Granier, C., 2022. High-resolution](#)
603 [biogenic global emission inventory for the time period 2000–2019 for air quality modelling. Earth Syst. Sci. Data.](#)
604 [14, 251–270.](#)

605 Sinha, B.P. and Sinha, V., 2019. Source apportionment of volatile organic compounds in the northwest Indo-
606 Gangetic Plain using a positive matrix factorization model. Atmos. Chem. Phys. 19, 15467–15482.

607 [Song, M.D., Li, X., Yang, S.D., Yu, X.A., Zhou, S.X., Yang, Y.M., Chen, S.Y., Dong, H.B., Liao, K.R., Chen,](#)
608 [Q., Lu, K.D., Zhang, N.N., Cao, J.J., Zeng, L.M., Zhang, Y.H., 2021. Spatiotemporal variation, sources, and](#)
609 [secondary transformation potential of volatile organic compounds in Xi'an, China. Atmos. Chem. Phys. 21,](#)
610 [4939–4958.](#)

611 Stavrou, T., Müller, J.-F., Bauwens, M., De Smedt, I., Van Roozendaal, M., Guenther, A., Wild, M., Xia, X.,
612 2014. Isoprene emissions over Asia 1979–2012: impact of climate and land-use changes. Atmos. Chem. Phys.,
613 14, 4587–4605, <https://doi.org/10.5194/acp-14-4587-2014>.

614 Sun, W., Wang, D., Yao, L., Fu, H., Fu, Q., Wang, H., Li, Q., Wang, L., Yang, X., Xian, A. (2019) Chemistry-
615 triggered events of PM_{2.5} explosive growth during late autumn and winter in Shanghai, China. Environmental
616 pollution_ 254, 112864.

617 [Sun, Y. L., He, Y., Kuang, Y., Xu, W. Y., Song, S. J., Ma, N., Tao, J. C., Cheng, P., Wu, C., Su, H., Cheng, Y. F.,](#)

618 [Xie, C. H., Chen, C., Lei, L., Qiu, Y. M., Fu, P. Q., Croteau, P., Worsnop, D. R., 2020. Chemical Differences](#)
619 [Between PM₁ and PM_{2.5} in Highly Polluted Environment and Implications in Air Pollution Studies. Geophys.](#)
620 [Res. Lett. 47, No. e2019GL086288.](#)

621 [Tsai, S. M., Zhang, J. J., Smith, K. R., Ma, Y., Rasmussen, R. A., Khalil, M. A. K., 2003. Characterization of](#)
622 [Non-methane Hydrocarbons Emitted from Various Cookstoves Used in China. Environ. Sci. Technol. 37, 2869–](#)
623 [2877.](#)

624 [Tong, Y., Pospisilova, V., Qi, L., Duan, J., Gu, Y., Kumar, V., Rai, P., Stefenelli, G., Wang, L., Wang, Y., Zhong,](#)
625 [H., Baltensperger, U., Cao, J., Huang, R.J., Prévôt, A. S. H., Slowik, J. G., 2021. Quantification of solid fuel](#)
626 [combustion and aqueous chemistry contributions to secondary organic aerosol during wintertime haze events in](#)
627 [Beijing. Atmos. Chem. Phys. 21, 9859–9886.](#)

628 Wang, H.L., Chen, C.H., Wang, Q., Huang, C., Su, L.Y., Huang, H.Y., Lou, S.R., Zhou, M., Li, L., Qiao, L.P.,
629 Wang, Y.H., 2013^a. Chemical loss of volatile organic compounds and its impact on the source analysis through
630 a two-year continuous measurement. Atmos. Environ. 80, 488–498.

631 [Wang, M., Shao, M., Lu, S.H., Yang, Y.D., Chen, W.T., 2013b. Evidence of coal combustion contribution to](#)
632 [ambient VOCs during winter in Beijing. Chin. Chem. Lett. 24, 829–832.](#)

633 [Wang, J., Jin, L., Gao, J., Shi, J., Zhao, Y., Liu, S., Jin, T., Bai, Z., Wu, C.Y., 2013c. Investigation of speciated](#)
634 [VOC in gasoline vehicular exhaust under ECE and EUDC test cycles. Sci. Total Environ. 445, 110–116.](#)

635 Wang, Y.S., Yao, L., Wang, L.L., Liu, Z.R., Ji, D.S., Tang, G. Q., Zhang, J.K., Sun, Y., Hu, B., Xin, J.Y., 2014^a.
636 Mechanism for the formation of the January 2013 heavy haze pollution episode over central and eastern China.
637 Sci. China Earth Sci. 57, 14–25, <https://doi.org/10.1007/s11430-013-4773-4>.

638 [Wang, H., Qiao, Y., Chen, C., Lu, J., Dai, H., Qiao, L., Lou, S., Huang, C., Li, L., Jing, S., Wu, J., 2014b. Source](#)
639 [Profiles and Chemical Reactivity of Volatile Organic Compounds from Solvent Use in Shanghai, China. *Aerosol*](#)
640 [Air Qual. Res. 14, 301–310.](#)

641 Wang, T., Xue, L., Brimblecombe, P., Lam, Y.F., Li, L., Zhang, L., 2017. Ozone Pollution in China: A Review
642 of Concentrations, Meteorological Influences, Chemical Precursors, and Effects. *Sci. Total Environ.* 575,
643 1582–1596.

644 Wang, J., Yang, Y., Zhang, Y., Niu, T., Jiang, X., Wang, Y., Che, H., 2019. Influence of meteorological
645 conditions on explosive increase in O₃ concentration in troposphere. *Sci. Total Environ.* 652, 1228-1241.

646 Wang, M, L., Li, S.Y., Zhu, R.C., Zhang, R.Q., Zu, L., Wang, Y.J., Bao, X.F., 2020. On-road tailpipe emission
647 characteristics and ozone formation potentials of VOCs from gasoline, diesel and liquefied petroleum gas fueled
648 vehicles. *Atmos. Environ.* 223, 117294.

649 Warneke, C., McKeen, S. A., de Gouw, J. A., Goldan, P. D., Kuster, W. C., Holloway, J. S., Williams, E. J.,
650 Lerner, B. M., Parrish, D. D., Trainer, M., Fehsenfeld, F. C., Kato, S., Atlas, E. L., Baker, A., Blake, D. R., 2007.
651 Determination of urban volatile organic compound emission ratios and comparison with an emissions database.
652 *J. Geophys. Res.* 112, D10S47, <https://doi.org/10.1029/2006jd007930>.

653 [Wu, R.R., Li, J., Hao, Y.F., Li, Y.Q., Zeng, L.M., Xie, S.D., 2016. Evolution process and sources of ambient](#)
654 [volatile organic compounds during a severe haze event in Beijing, China. *Sci. Total. Environ.* 560-561, 62-72.](#)

655 Wu, R. and Xie, S., 2018. Spatial Distribution of Secondary Organic Aerosol Formation Potential in China
656 Derived from Speciated Anthropogenic Volatile Organic Compound Emissions, *Environ. Sci. Technol.* 52,
657 8146–8156, <https://doi.org/10.1021/acs.est.8b01269>.

658 Xing, J., Wang, S. X., Jang, C., Zhu, Y., Hao, J. M., 2011. Nonlinear response of ozone to precursor emission
659 changes in China: a modeling study using response surface methodology. *Atmos. Chem. Phys.* 11, 5027–5044;
660 <https://doi.org/10.5194/acp-11-5027-2011>.

661 [Xu, W., Sun, Y., Wang, Q., Zhao, J., Wang, J., Ge, X., Xie, C., Zhou, W., Du, W., Li, J., Fu, P., Wang, Z., Worsnop,](#)
662 [D.R., Coe, H., 2019. Changes in Aerosol Chemistry From 2014 to 2016 in Winter in Beijing: Insights From High-](#)
663 [Resolution Aerosol Mass Spectrometry. *J. Geophys. Res.: Atmos.* 124 \(2\), 1132–1147](#)

664 Xu, Q., Wang, S., Jiang, J., 2019. Nitrate dominates the chemical composition of PM_{2.5} during haze event in
665 Beijing, China. *Sci. Total. Environ.* 689:1293-1303.

666 Xue, Y., Ho, S. S. H., Huang, Y., Li, B., Wang, L., Dai, W., Cao, J., Lee, S., 2017. Source apportionment of
667 VOCs and their impacts on surface ozone in an industry city of Baoji, Northwestern China. *Sci. Rep.* 7, 9979,
668 <https://doi.org/10.1038/s41598-017-10631-4>.

669 Xue, T., Zheng, Y., Geng, G., Xiao, Q., Meng, X., Wang, M., Li, X., Wu, N., Zhang, Q., Zhu, T., 2020a.
670 Estimating Spatiotemporal Variation in Ambient Ozone Exposure during 2013–2017 Using a Data-Fusion Model.
671 *Environ Sci. Technol.* 54, 14877-14888.

672 Xue, Y., Huang, Y., Ho, S.S.H., Chen, L., Wang, L., Lee, S., Cao, J., 2020b. Origin and transformation of ambient
673 volatile organic compounds during a dust-to-haze episode in northwest China. *Atmos. Chem. Phys.* 20, 5425-
674 5436.

675 [Yan, Y., Peng, L., Li, R., Li, Y., Li, L., Bai, H., 2017. Concentration, ozone formation potential and source analysis](#)
676 [of volatile organic compounds \(VOCs\) in a thermal power station centralized area: A study in Shuozhou, China.](#)
677 [*Environ. Pollut.* 223, 295–304.](#)

678 Yang, W.Q., Zhang, Y.L., Wang, X.M., Li, S., Zhu, M., Yu, Q.Q., Li, G.H., Huang, Z.H., Zhang, H.N., Wu, Z.F.,
679 Song, W., Tan, J.H., Shao, M., 2018. Volatile organic compounds at a rural site in Beijing: influence of temporary
680 emission control and wintertime heating. *Atmos. Chem. Phys.* 18, 12663–12682.

681 [Yao, Y.C., Tsai, J.H., Wang, I.T., 2013. Emissionsof gaseous pollutant from motorcycle powered byethanol-](#)
682 [gasoline blend. *Appl. Energy.* 102, 93–100.](#)

683 [Yao, Z., Wu, B., Shen, X., Cao, X., Jiang, X., Ye, Y., He, K., 2015. On-road emission characteristics of VOCsfrom](#)
684 [rural vehicles and their ozone formation potential in Beijing, China. *Atmos. Environ.* 105, 91–96.](#)

685 Yao, L., Wang, D., Fu, Q., Qiao, L., Wang, H., Li, L., Sun, W., Li, Q., Wang, L., Yang, X., 2019. The effects of
686 firework regulation on air quality and public health during the Chinese Spring Festival from 2013 to 2017 in a
687 Chinese megacity. *Environ Int.* 126, 96-106.

688 [Yuan, B., Shao, M., Lu, S., Wang, B., 2010. Source profiles of volatile organic compounds associated with solvent](#)
689 [use in Beijing, China. *Atmos. Environ.* 44, 1919–1926.](#)

690 Zhai, S., Jacob, D.J., Wang, X., Shen, L., Li, K., Zhang, Y., Gui, K., Zhao, T., Liao, H., 2019. Fine particulate
691 matter (PM_{2.5}) trends in China, 2013–2018: separating contributions from anthropogenic emissions and
692 meteorology, *Atmos. Chem. Phys.* 19, 11031– 11041, <https://doi.org/10.5194/acp-19-11031-2019>.

693 [Zhang, Y., Wang, X., Zhang, Z., Lu, S., Shao, M., Lee, F.S. C., Yu, J., 2013. Species profiles and normalized re](#)
694 [activity of volatile organic compounds from gasoline evaporation in China. *Atmos. Environ.* 79, 110–118.](#)

695 Zhang, X., Xue, Z., Li, H., Yan, L., Yang, Y., Wang, Y., Duan, J., Li, L., Chai, F., Cheng, M., Zhang, W., 2017^a.
696 Ambient volatile organic compounds pollution in China. *J Environ. Sci.*, 55, 69-75, 10.1016/j.jes.2016.05.036.

697 ~~Zhang, H., Li, H., Zhang, Q., Zhang, Y., Zhang, W., Wang, X., Bi, F., Chai, F., Gao, J., Meng, L., Yang, T.,~~
698 ~~Chen, Y., Cheng, Q., Xia, F., 2017b. Atmospheric Volatile Organic Compounds in a Typical Urban Area of~~
699 ~~Beijing: Pollution Characterization, Health Risk Assessment and Source Apportionment. Atmosphere 8, 61.~~

700 Zhang, Y., Li, R., Fu, H., Zhou, D., Chen, J., 2018. Observation and analysis of atmospheric volatile organic
701 compounds in a typical petrochemical area in Yangtze River Delta, China. J. Environ. Sci. 71, 233-248.

702 Zhao, D., Liu, G., Xin, J., Quan, J., Wang, Y., Wang, X., 2020. Haze pollution under a high atmospheric
703 oxidization capacity in summer in Beijing: insights into formation mechanism of atmospheric physicochemical
704 processes. Atmos. Chem. Phys. 20, 4575-4592.

705 Zhao, Q.Y., Bi, J., Liu, Q., Ling, Z.H., Shen, G.F., Chen, F., Qiao, Y.Z., Li, C.Y., Ma, Z.W., 2020. Sources of
706 volatile organic compounds and policy implications for regional ozone pollution control in an urban location of
707 Nanjing, East China. Atmos. Chem. Phys. 20, 3905–3919.

708 ~~Zheng, J., Yu, Y., Mo, Z., Zhang, Z., Wang, X., Yin, S., Peng, K., Yang, Y., Feng, X., Cai, H., 2013. Industrial~~
709 ~~sector-based volatile organic compound (VOC) source profiles measured in manufacturing facilities in the Pearl~~
710 ~~River Delta, China. Sci. Total Environ. 456, 127–136.~~

711 Zheng, H., Kong, S., Xing, X., Mao, Y., Hu, T., Ding, Y., Li, G., Liu, D., Li, S., Qi, S., 2018. Monitoring of
712 volatile organic compounds (VOCs) from an oil and gas station in northwest China for 1 year. Atmos. Chem.
713 Phys. 18, 4567-4595.

714

Figure captions

715

716 **Figure 1.** Time series of meteorological parameters and levels of air pollutants during the sampling
717 period.

718 **Figure 2.** Comparison of the concentration and composition of major chemical groups observed in
719 2019 (this study), 2016 (Liu et al., 2020) and 2014 (Li et al., 2015).

720 **Figure 3.** Comparison of major meteorological parameters and air pollutants on clean and polluted
721 days.

722 **Figure 4.** Statistic decomposition of meteorological and emission contribution to O₃ and PM_{2.5}
723 levels during different periods.

724 **Figure 5.** OFP and SOAFP by chemical groups during different periods.

725 **Figure 6.** Ratios of i/n-pentane and toluene/benzene at different PM_{2.5} and O₃ levels.

726 **Figure 67.** Source profiles of VOCs identified using the PMF model and the relative contributions
727 of the individual VOC species.

728 **Figure 78.** Contributions of each source to VOCs during different periods.

729 **Figure 89.** Contributions of each source to OFP and SOAFP during different periods.

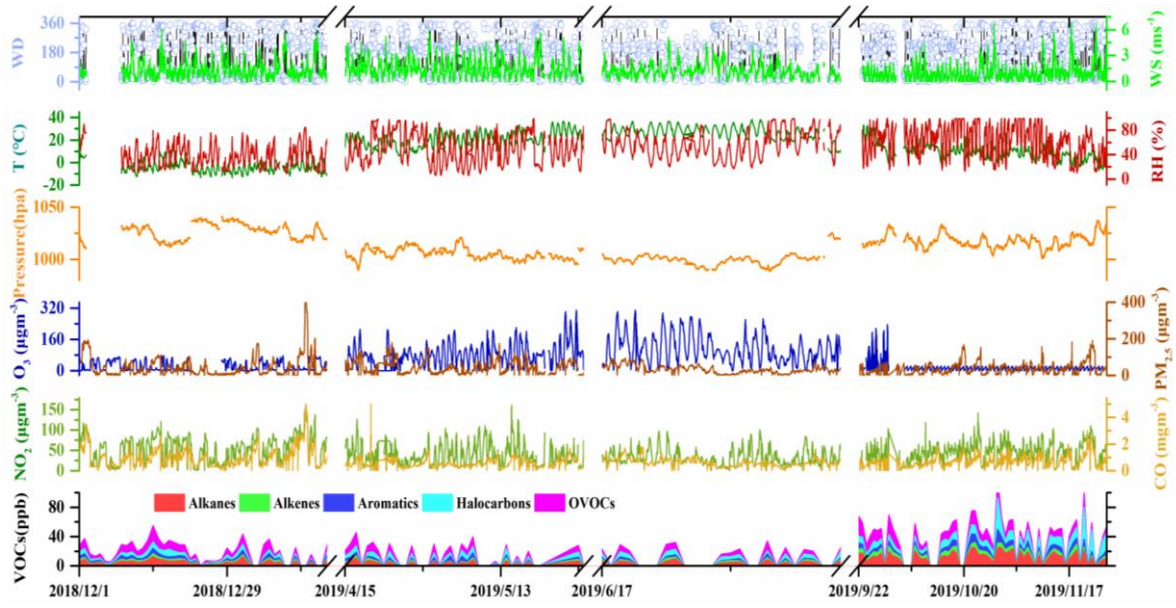
730 **Figure 910.** OFP values of the dominant VOC species in the different source categories ~~during for~~
731 the ~~on-O₃ polluted-pollution~~ (a) and ~~clean-compliance~~ (b) days of the ~~high-O₃-polluted~~ months, and
732 SOAFP values ~~on for the PM_{2.5} pollution-polluted~~ (c) and ~~complianceclean~~ (d) days of the ~~high-~~
733 PM_{2.5}-~~polluted~~ months.

734 **Figure 10.** ~~Backward trajectory cluster analysis (24 h) and PSCF analysis during different periods:~~
735 ~~(a) polluted days of the high-O₃ months, (b) clean days of the high-O₃ months, (c) low-O₃ months.~~

736 **Figure 11.** ~~Backward trajectory cluster analysis (24 h) and PSCF analysis during different periods:~~

737 ~~(a) polluted days of the high PM_{2.5} months, (b) clean days of the high PM_{2.5} months, (c) low PM_{2.5}~~
738 ~~months.~~

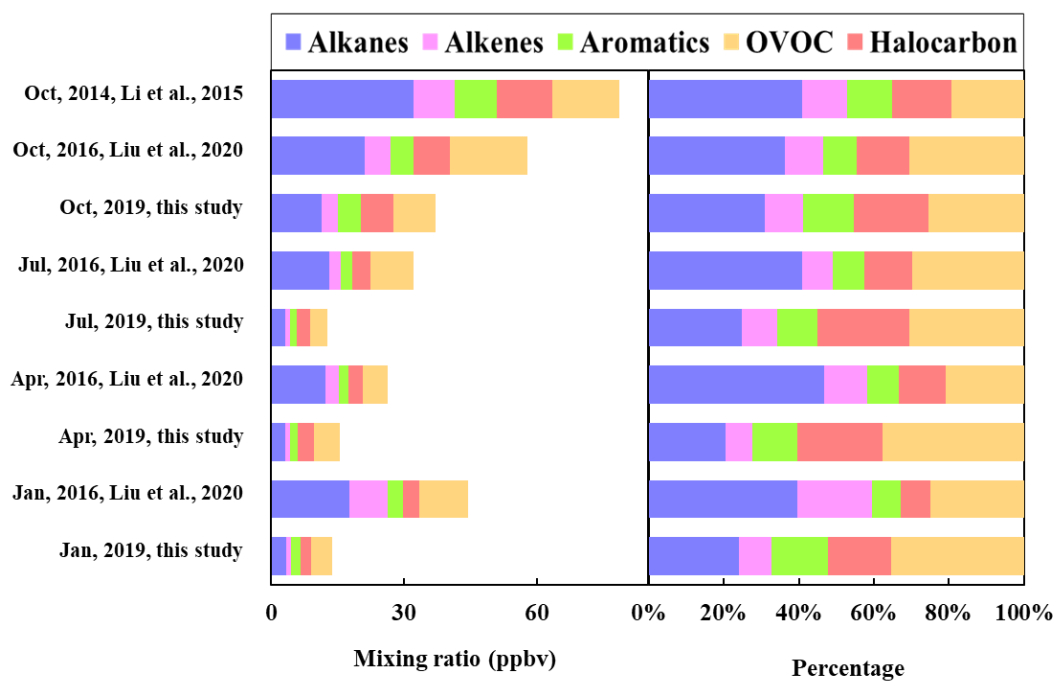
Fig. 1.



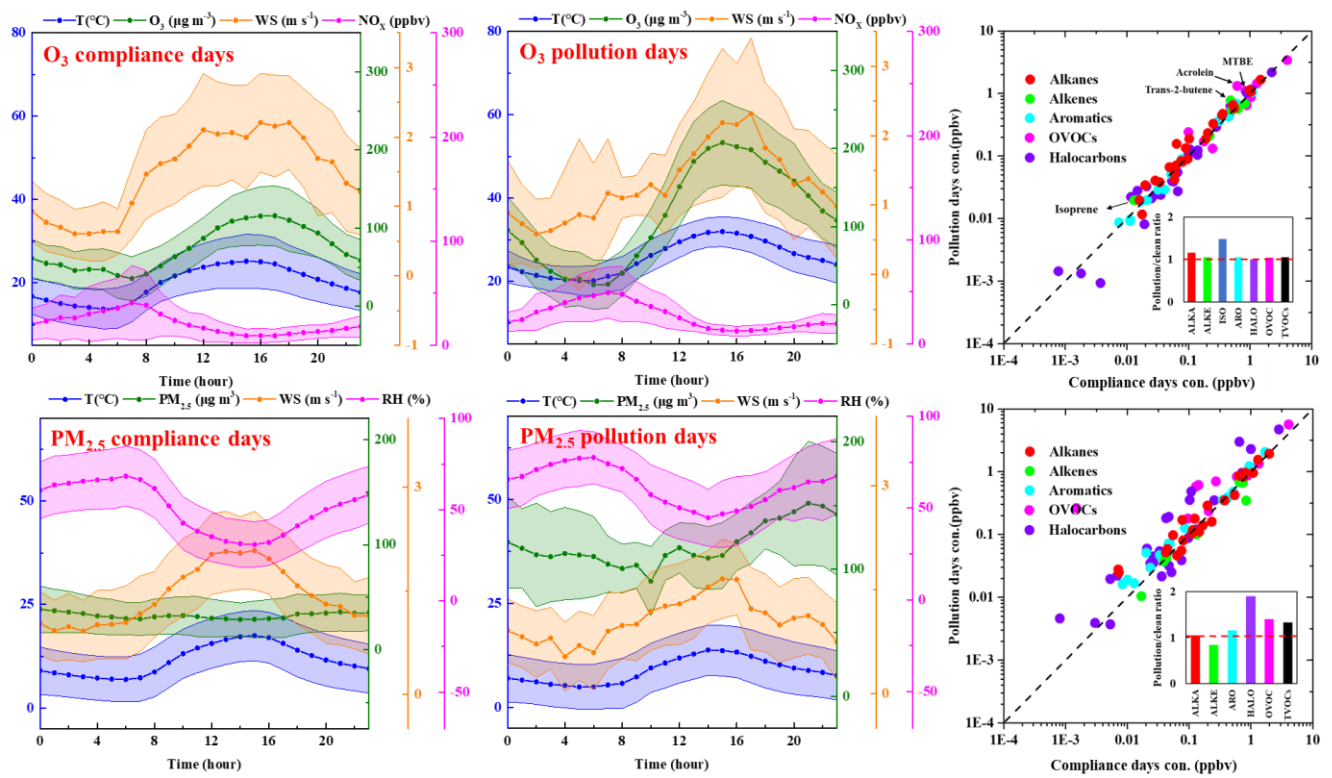
742

743

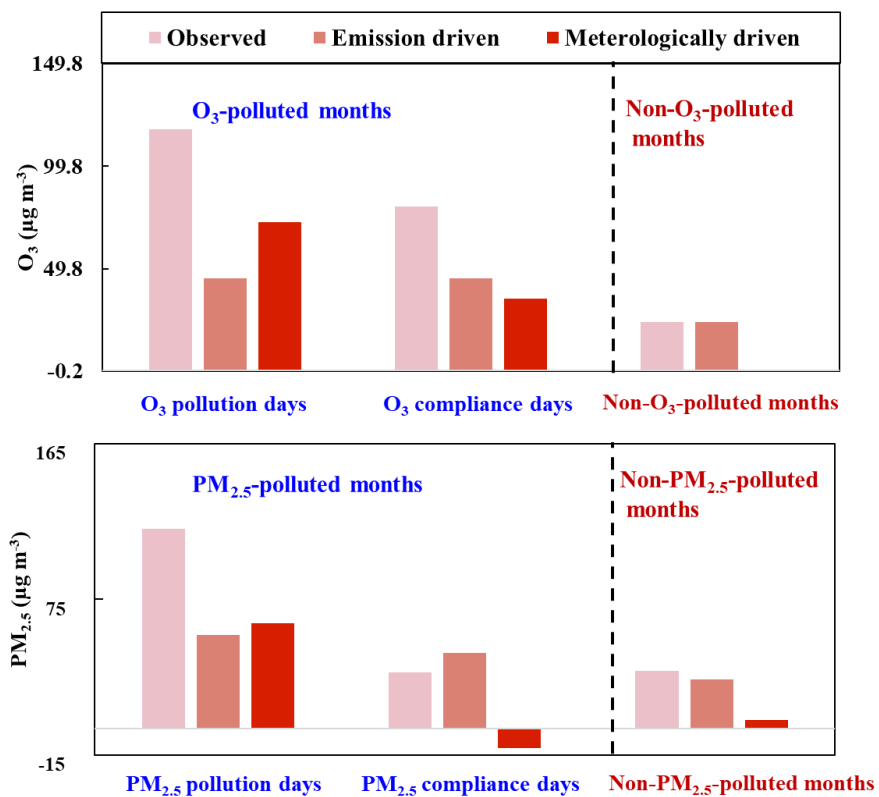
744 **Figure 2.**



745



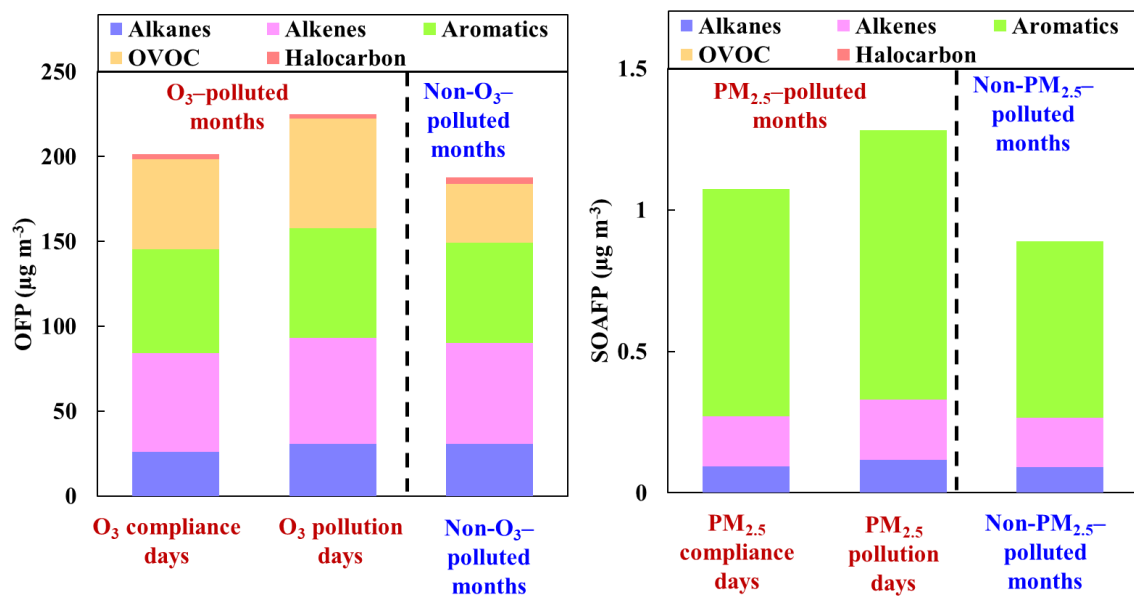
749 **Fig. 4**



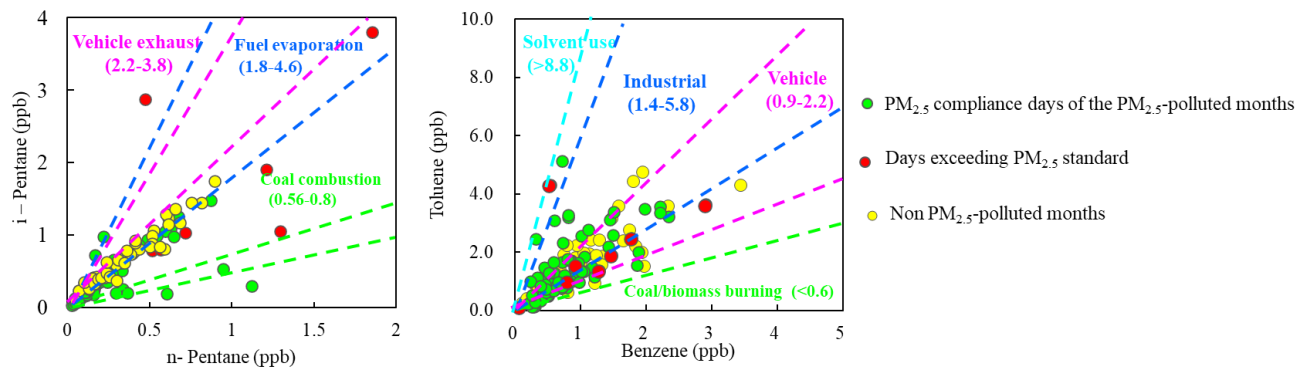
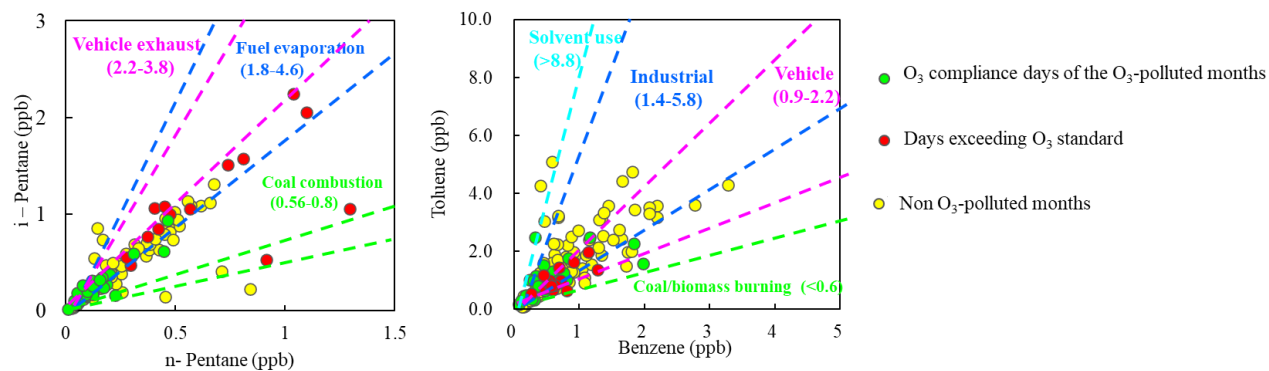
753

Fig. 5

754

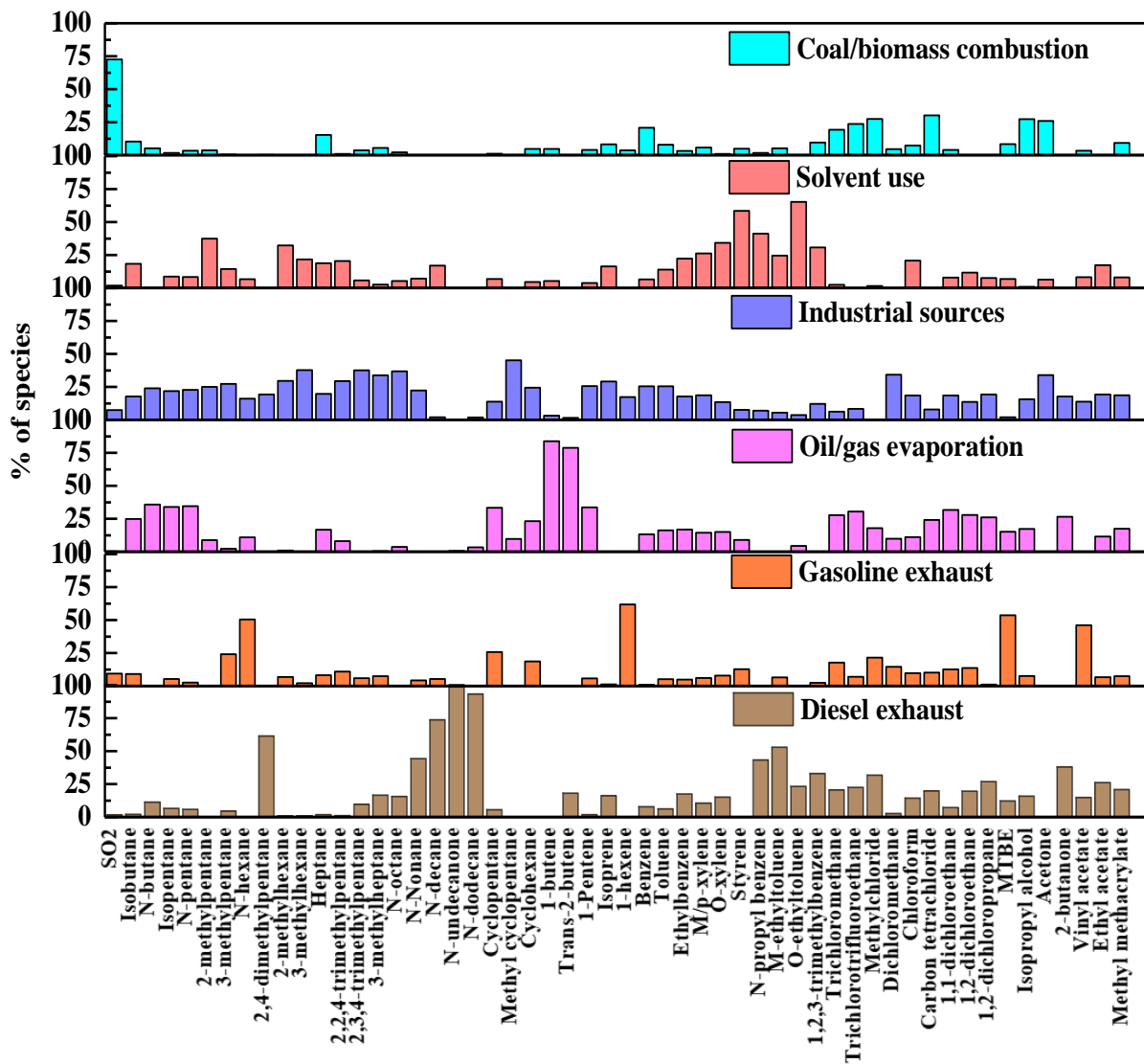


755

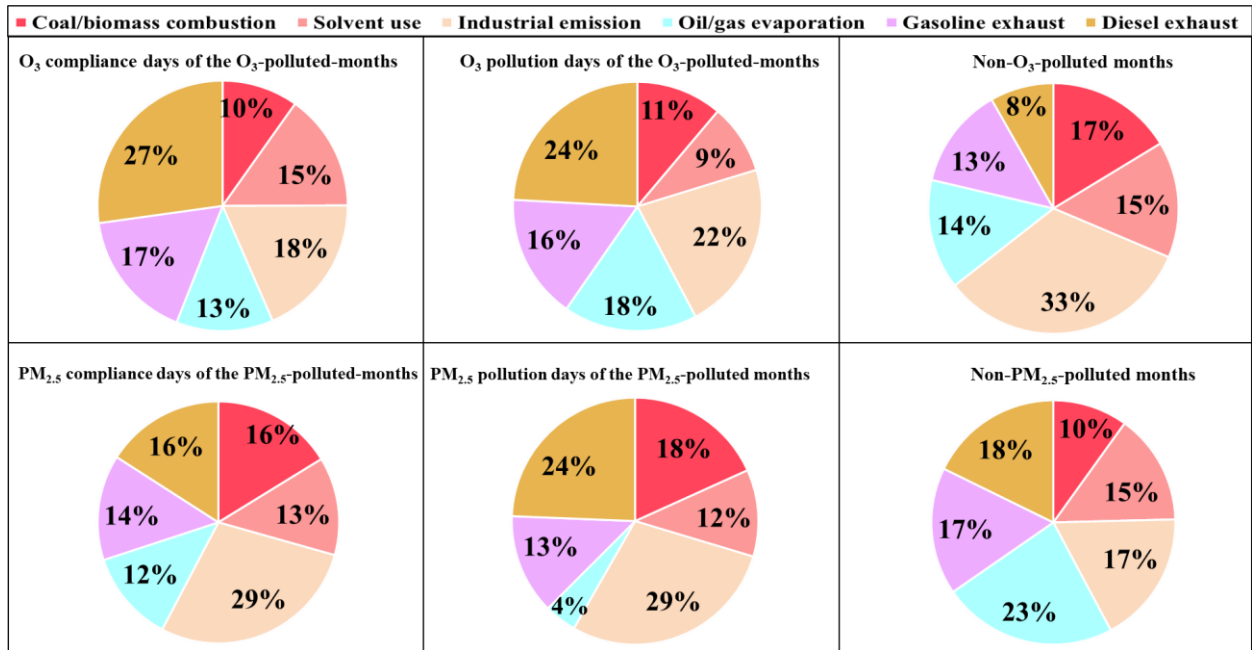
Fig. 6**Ratios of *i/n*-pentane and toluene/benzene at different PM_{2.5} levels****Ratios of *i/n*-pentane and toluene/benzene at different O₃ levels**

758
759
760
761
762

Fig. 67.



763 **Fig. 78**



768 **Fig. 89**

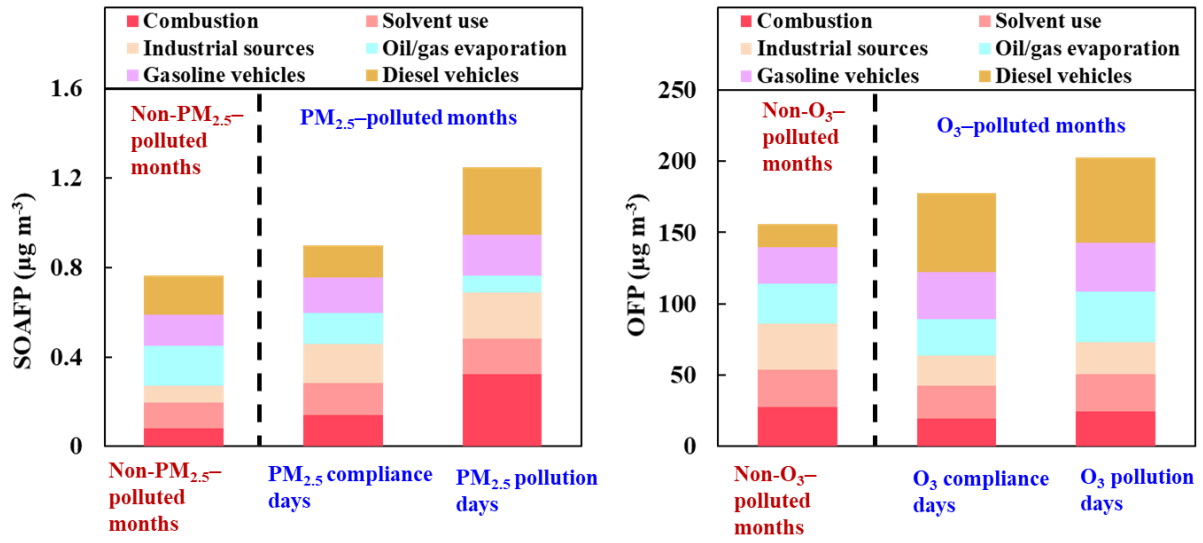


Fig. 910

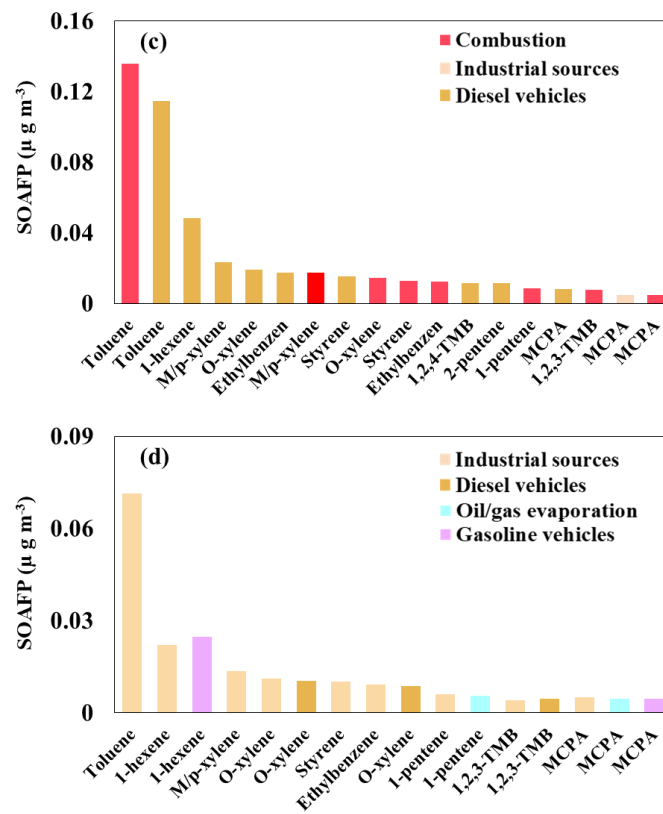
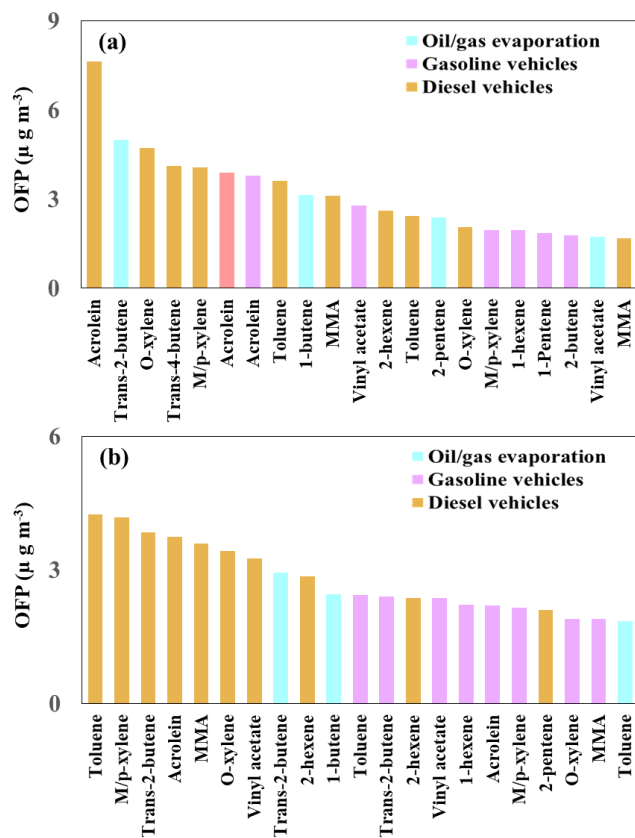


Fig. 10

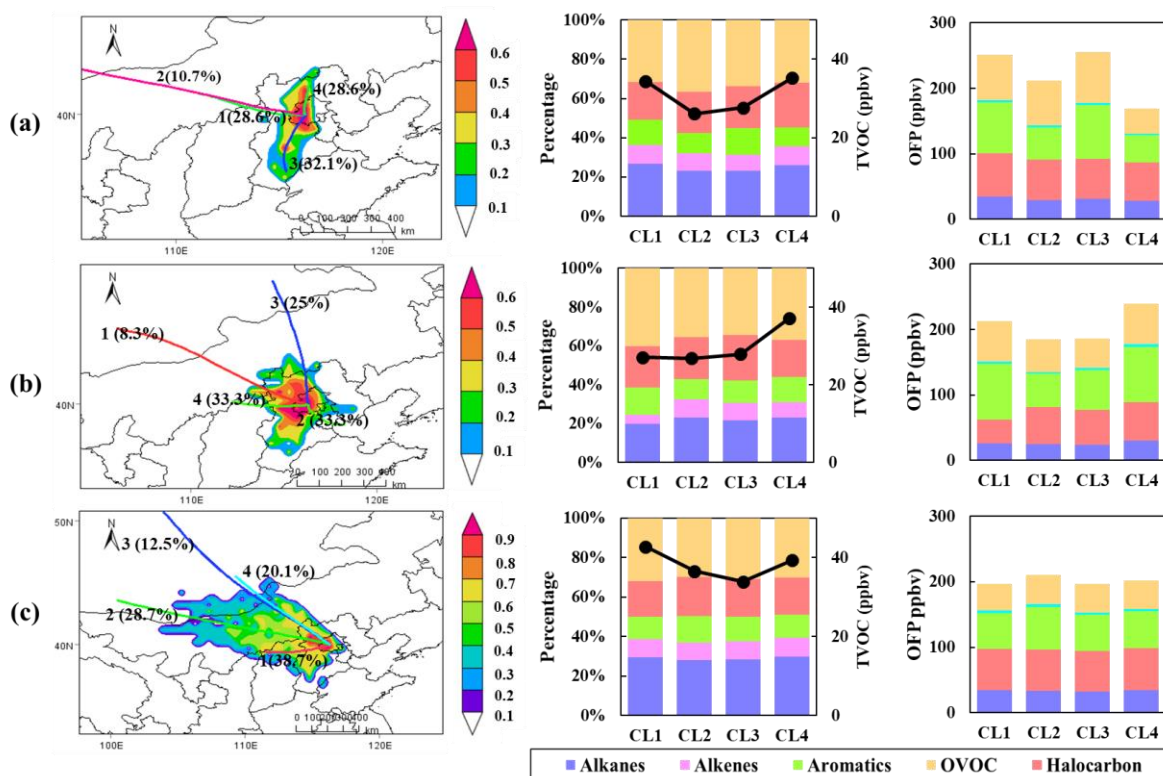


Fig. 11

